CHARACTERIZATION OF CARBON NANOTUBES GROWN BY CHEMICAL VAPOUR DEPOSITION

by

Muhammad Shafiq Ahmed

A Thesis Submitted in Partial Fulfillment
of the Requirements for the Degree of

Master of Science

in

The Faculty of Science

Materials Science Program

University of Ontario Institute of Technology

August 2009

© M.S.Ahmed, 2009

CERTIFICATE OF APPROVAL

Abstract

Carbon nanotubes (CNTs), discovered by Ijima in 1991, are one of the allotropes of carbon, and can be described as cylinders of graphene sheet capped by hemi-fullerenes. CNTs have excellent electrical, mechanical, thermal and optical properties and very small size. Due to their unique properties and small size, CNTs have a great potential for use in electronics, medical applications, field emission devices (displays, scanning and electron probes/microscopes) and reinforced composites. CNTs can be grown by different methods from a number of carbon sources such as graphite, CO, C_2H_4, CH_4 and camphor. Under certain conditions, a metallic catalyst is used to initiate the growth. The three main methods used to grow CNTs are: Arc-discharge, laser ablation (LA) and chemical vapour deposition (CVD). In the present work CNTs were grown from a mixture of camphor ($C_{10}H_{16}O$) and ferrocene ($C_{10}H_{10}Fe$) using Chemical Vapour Deposition (CVD) and argon was used as a carrier gas. The iron particles from ferrocene acted as catalysts for growth. The substrates used for the growth of CNTs were crystalline Si and SiO_2 (Quartz) placed in a quartz tube in a horizontal furnace. Several parameters have been found to affect the CNT growth process. The effects of three parameters: growth temperature, carrier gas (Ar) flow rate and catalyst concentration were investigated in the present work in order to optimize the growth conditions with a simple and economical CVD setup. The samples were characterized using electron microscopy (EM), thermogravimetirc analysis (TGA), Raman and FTIR spectroscopy techniques. It was found that the quality and yield of the CNTs were best at 800°C growth temperature, 80sccm flow rate and 4% catalyst concentration.

Acknowledgments

I would like to sincerely thank and honour all those who directly or indirectly helped and supported me in the completion of this work, especially:

My supervisor, Dr. Franco Gaspari, for his continuous support and guidance during this research work, my advisory committee members, Dr. William Smith and Dr. Brad Easton, for their precious suggestions and help, Dr. Matthew Kaye, Faculty of Energy Systems and Nuclear Science, who has generously allowed me to use the quartz tube for CVD setup, Dr. Gianluigi Botton for teaching and allowing me to use SEM and TEM facilities at Canadian Center for Electron Microscopy at McMaster University in Hamilton, ON. Mr. Fred Pearson for his help in getting TEM data, Dr. Glynis de Silveira and Chris Butcher for their help in getting SEM data, Dr. Andrew Vreugdenhil, for teaching and allowing me to use Raman Microscope in his laboratory at Trent University in Peterborough, ON, Andrew Pedersen for all of his technical support and help in arranging CVD setup, Nicole De Almeida for explaining me the use of TGA setup and Timothy V. Teatro for a wonderful company during our graduate study at University of Ontario Institute of Technology (UOIT).

Thanks to all of the teaching Faculty involved in the Materials Science Program at both UOIT and Trent Universities and staff in the Faculty of Science, UOIT, for their support and cooperation during the whole study period.

Table of Contents

4   **EXPERIMENTAL DETAILS**

5   **RESULTS AND DISCUSSIONS**

List of Tables

List of Figures

x

List of Abbreviations

CNT   Carbon Nanotube

SWNT   Single Wall Carbon Nanotube

MWNT   Multi Wall Carbon Nanotube

VACNT   Vertically Aligned Carbon Nanotube

CNF   Carbon Nano Fiber

SEM   Scanning Electron Microscope

TEM   Transmission Electron Microscope

HRTEM   High Resolution Transmission Electron Microscope

HiPCO   High Pressure Carbon mono Oxide

EDP   Electron Diffraction Pattern

EDX   Energy Dispersive X-ray

EELS   Electron Energy Loss Spectroscopy

FTIR   Fourier Transform Infrared Spectrum

HATR   Horizontal Attenuated Total Reflection

UV-vis   Ultraviolet and visible

NIR   Near-infrared

TGA   Thermo-Gravimeteric Analysis

DTA   Differential Thermal Analysis

DSC   Differential Scanning Calorimetery

DOS   Density of States

CVD   Chemical Vapor Deposition

PLV	Pulsed Laser Vaporization
LA	Laser Ablation
RBM	Radial Breathing Mode
HEM	High Energy Mode
C_h	Chiral vector of carbon nanotube
GPa	Giga Pascal (10^9 Pascal)

Chapter 1

INTRODUCTION

1.1 Carbon

The element Carbon belongs to group IV in the periodic table and has an atomic number of 6. Elemental carbon occurs in different solid forms. The stable low pressure and low temperature phase is called graphite, whose structure consists of planar hexagonal networked layers of carbon atoms. The high pressure and high temperature form of carbon is called diamond, which consists of tetrahedral network of carbon atoms forming a face centered cubic (f.c.c.) lattice. A closed cage form is called a fullerene and a tubular form is called a carbon nanotube. The phase diagram of carbon is shown in Fig. 1.1. A carbon atom has six electrons; two of them fill the $1s$ orbital and the remaining four electrons fill the sp^3, sp^2 or sp hybrid orbital. Diamond has sp^3 hybrid orbitals which make four equivalent σ covalent bonds to connect to four other carbon atoms and form the tetrahedral structure. The electrons within diamond are tightly held within the bonds among the carbon atoms. Diamond absorbs light in the ultraviolet region but not in the visible or infrared region, so pure diamond appears clear to human eyes. In graphite, three outer-shell electrons of each carbon atom occupy the planar sp^2 hybrid orbital to form three in-plane σ bonds, and one electron makes an out-of-plane π bond. This makes a planar hexagonal network of carbon atoms. Parallel hexagonal networks of carbon atoms are held together at certain spacing by the van der Waals force. The weak van der Waals interaction among graphite sheets makes graphite soft and ideal as a lubricant because the sheets can easily glide over each other. Graphite is stronger in-plane than

diamond (due to strong σ bonds) and because of the out-of-plane π bond it is thermally and electrically conductive. The loose π electron absorbs light in the visible range and causes the graphite to appear black [1,2].
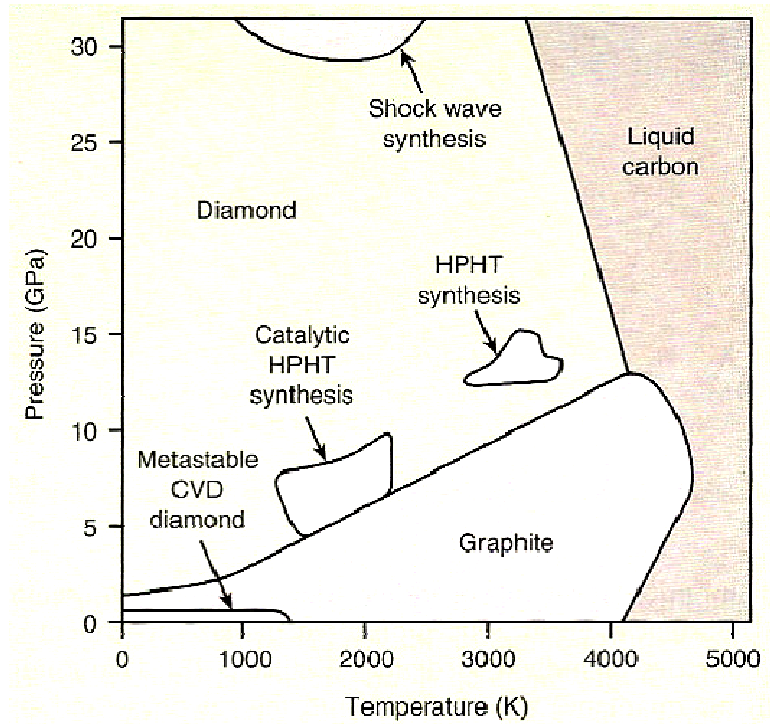
Figure 1.1 The phase diagram of carbon materials, reprinted with permission [4].

1.2 Carbon Nanotubes (CNTs)

A carbon nanotube (CNT) can be viewed as a hollow cylinder formed by rolling graphite sheets. Chemical bonding in nanotubes is sp^2, however rehybridization of bonds takes place due to curvature, causing the three σ bonds to slightly shift out of plane; for compensation, the π orbital is more delocalized outside the tube. This rehybridization gives the nanotubes extraordinary electronic, mechanical, chemical, thermal, magnetic,

and optical properties and makes them mechanically stronger, electrically and thermally more conductive, and chemically more active than graphite. This rehybridization also allows for topological defects, such as pentagons and heptagons, to be incorporated into the hexagonal network, to form capped bent, toroidal and helical nanotubes. Fullerene (C_{60}) is a closed cage structure made up of 60 atoms of carbon in the form of a hollow sphere whose surface consists of 20 hexagons and 12 pentagons. The bonding is also sp^2 with more rehybridization character because of high curvature [2]. All these forms are shown in Fig. 1.2(a).
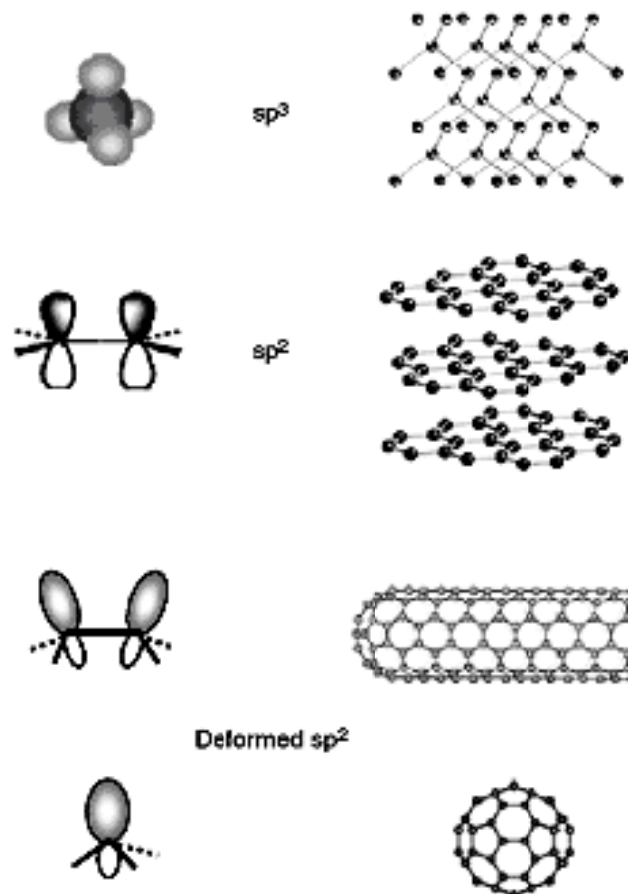
Figure 1.2 Bonding structures of diamond, graphite, nanotubes, and fullerenes, reprinted with permission [2].

Carbon nanotubes were discovered in 1991 by Iijima [3] while experimenting on fullerenes. CNTs can be single wall (SW) or multi wall (MW). A SWCNT consists only of a single wall of graphene sheet with one atomic layer rolled to form a tube while a MWCNT is formed from 2 to several tens of graphene sheets rolled into concentric tube structures, as shown in Fig. 1.3. MWCNTs have diameters up to 100nm, above which they are called carbon nano fibers (CNFs) [8].

SWCNT   MWCNT

a   b
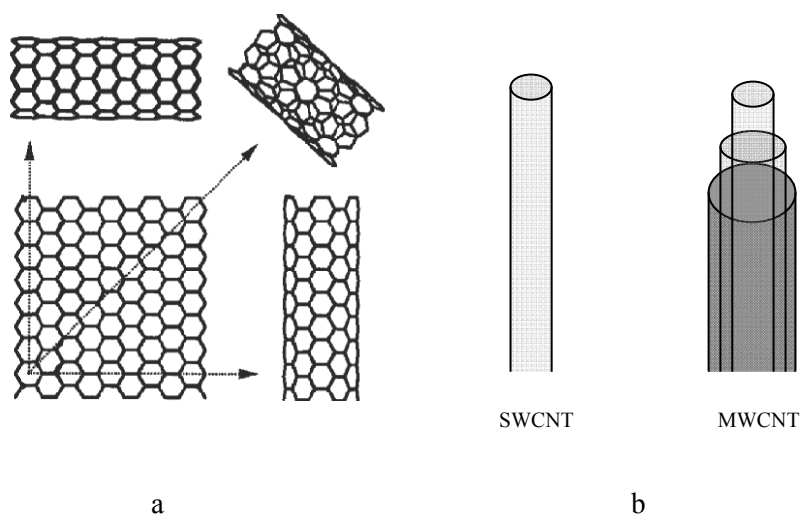
Figure 1.3 (a) Graphical representations of morphologies projected from the graphene sheet, reprinted with permission [2], (b) schematic of SWCNT and MWCNT.

More research has been done on single wall nanotubes (SWCNTs) due to their well defined and simple structure. SWCNTs have three basic geometrical forms; armchair, zigzag and chiral as presented in Fig. 1.3(b). SWCNTs are completely described (except for their length) by a single vector *C* (called chiral vector). Two atoms in a planar graphene sheet are chosen and one is used as origin. The chiral vector *C* is pointed from the first atom toward the second one (Fig. 1.4) and is defined by the relation:

$$C = na_1 + ma_2 \qquad\qquad (1)$$

Where n and m are integers, a1 and a2 the unit cell vectors of the two-dimensional lattice formed by the graphene sheets. The direction of the nanotube axis is perpendicular to this chiral vector [5].
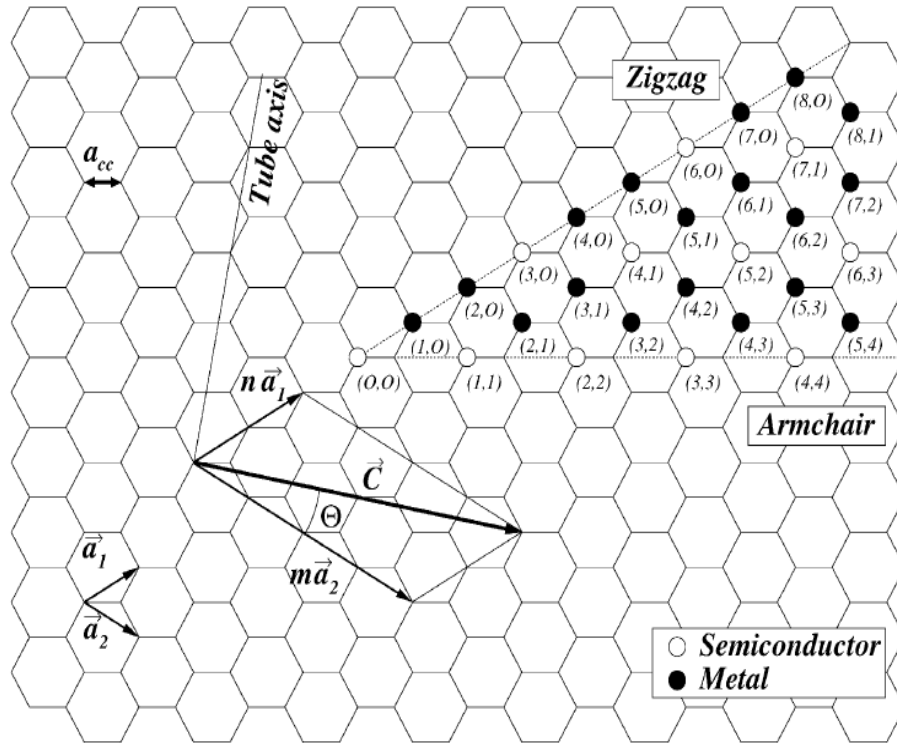
Figure 1.4 Chiral vector **C** and chiral angle θ definition for a (2, 4) nanotube on graphene sheet a_1 and a_2 are the unit cell vectors of the two-dimensional hexagonal graphene sheet. The chiral angle θ is the angle between the chiral vector **C** and the zigzag axis, reprinted with permission [5].

The length of the chiral vector **C** is the circumference of the nanotube and is given by the corresponding relationship:

$$c = |C| = a\,(n^2 + nm + m^2)^{1/2} \qquad\qquad (2)$$

where *a* is the length of the unit cell vector a_1 or a_2. This length *a* is related to the carbon-carbon bond length a_{cc} by the relation:

$$a = |a_1| = |a_2| = a_{cc}\sqrt{3}$$

(3)

For graphite, the carbon-carbon bond length is $a_{cc} = 0.1421$ nm. The same value is often used for nanotubes.

Using the circumferential length *c*, the diameter D of the carbon nanotube is thus given by the relation:

$$D = c/\pi$$

(4)

and the chiral angle θ (angle between the chiral vector and zigzag axis joining the carbon atoms) can be defined by:

$$\theta = \tan^{-1}\left(\frac{m\sqrt{3}}{m + 2n}\right)$$

(5)

Nanotubes are described by the pair of integers (*n,m*) which is related to the chiral vector. The value of (*n,m*) determines the chirality of the nanotube that affects the optical, mechanical and electronic properties. Three types of CNTs are revealed with these values:

when *n* = *m*, the nanotube is called "armchair" type ($\theta = 0°$)

when *m* = 0, then it is of the "zigzag" type ($\theta = 30°$)

otherwise, when *n* ≠ *m*, it is a "chiral" tube and θ takes a value between 0° and 30°.

Nanotubes with |*n* − *m*| = 3 (where *q* is an integer) are **metallic** and those with |*n* − *m*| = 3*q* ± 1 are **semiconducting**. The terminating cap of nanotube is formed from pentagons and hexagons. The smallest cap that fits on to the cylinder of the carbon tube is the C_{60} hemisphere [5].

1.3 Properties and Potential Application of Carbon nanotubes

CNTs consist of only one element, i.e. Carbon. This chemical simplicity allows physical properties to be calculated in detail for comparison with experimental results. The electronic properties of CNTs are unique in the way that the presence or absence of an energy gap depends on the way in which the carbon hexagons match up around the circumference of the tube. CNTs can be made to have either metallic or semiconducting properties by altering the tubes' geometrical structure (chirality) without adding any dopant into the system. Electronic and structural properties of carbon nanotubes are determined to a large extent by their nearly one dimensional structure [8]. CNTs have received a lot of attention and numerous ideas for their applications have been proposed since their discovery. Thanks to their remarkable physical properties, such as their high Young's modulus, high electrical conductivity and high aspect ratio. The potential applications of CNTs include: electronics (transistors, wires, interconnects), opto-electronics (light-emitting diodes, lasers), sensors, field emission devices (displays, scanning and electron probes/microscopes), batteries/fuel cells, fibers, reinforced composites, medical and biological applications, and hydrogen storage [9].

The most important properties of CNTs and some of their potential applications are stated below:

Electronic properties: Electronic properties of CNTs have received the greatest attention because of their high electrical and thermal conductivities. Depending on their chiral vector, carbon nanotubes with a small diameter are either semi-conducting or

metallic. The differences in conducting properties are caused by the molecular structure that results in a different band structure and a different band gap [6].

Optical properties: Defect-free nanotubes, offer direct band gap and well-defined band and sub-band structure, which are ideal for optical and optoelectronic applications. Optical spectra have been established for individual SWCNTs using fluorescence, and ultraviolet to the near infrared (UV-Vis-NIR) spectroscopic techniques. Theoretical studies have revealed that the optical activity of chiral nanotubes disappears if the nanotubes become larger [6]. Dai *et al.* [9] used the optical absorbance properties of SWCNTs to demonstrate the selective destruction of cancer cells. Cancer cells have many surface receptors for folate, so by noncovalently functionalizing SWCNTs with folate, SWCNTs were able to enter cancerous cells but not the receptor-free healthy ones. Near-infrared (NIR) light is harmless to the body, but with radiation from a NIR laser, the cells that internalized SWCNTs heated up to 70°C in two minutes and resulted in cell death.

Mechanical properties: Carbon nanotubes have a very large Young modulus in their axial direction. Sigma (σ) bonding is the strongest in nature, and thus a nanotube that is structured with all σ bonding is regarded as the ultimate fiber with the strength in its tube axis. Both experimental measurements and theoretical calculations agree that a nanotube is as stiff as or stiffer than diamond with the highest Young's modulus and tensile strength. Most theoretical calculations are carried out for perfect structures and give very consistent results [19].

In general, various types of defect-free nanotubes are stronger than graphite. This is mainly because the axial component of σ bonding is greatly increased when a graphite

sheet is rolled to form a tube. The Young's modulus is independent of tube chirality, but dependent on tube diameter. The Young's modulus for MWCNT is higher than a SWCNT, typically 1.1 to 1.3 TPa, determined both experimentally and theoretically. When many SWCNTs are held together in a bundle or a rope, the weak van der Waal force induces a strong shearing among the packed SWCNTs which decreases the Young's modulus. It is shown experimentally that the Young's modulus decreases from 1 TPa to 100 GPa when the diameter of a SWCNT bundle increases from 3 nm to 20 nm. The elastic response of a nanotube to deformation is also very remarkable. Most hard materials fail with a strain of 1% or less due to propagation of dislocations and defects. Both theory and experiment show that CNTs can sustain up to 15% tensile strain before fracture [2 and reference therein].

Chemical properties: The chemical reactivity of a CNT (compared with a graphene sheet) is enhanced as a direct result of the curvature of the CNT surface. Carbon nanotube reactivity is directly related to the pi-orbital mismatch caused by an increased curvature, so a smaller nanotube diameter results in increased reactivity. Open ends of the tube are also chemically reactive. Chemical modifications of either sidewalls or end caps have been reported. The modification of CNT is promising for use in applications such as sensors, polymer-CNT composites and coatings [6].

Thermal properties: CNTs have high thermal conductivity along the tube axis. The high thermal conductivity along the tube axis is shown in Fig. 1.5a. This allows for the use of CNTs in thermal management like, for instance, on chip cooling, as shown in Fig. 1.5b. The vertically aligned MWCNTs conduct heat along the length of the tube.
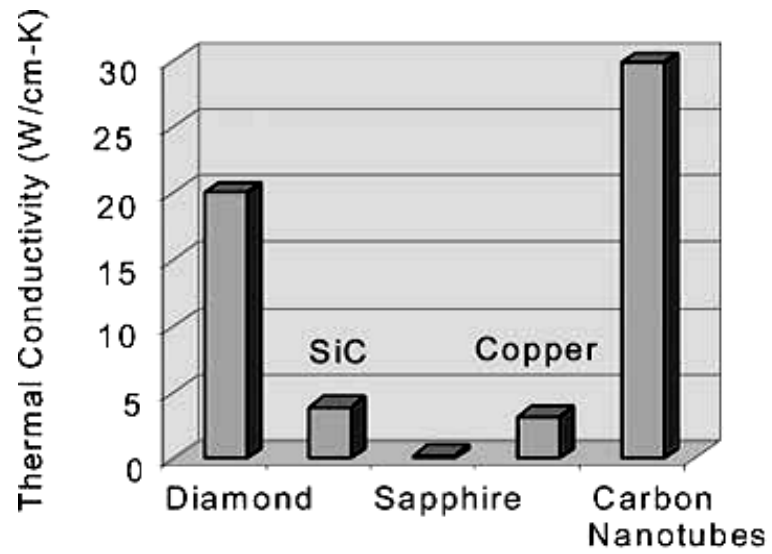
(a)
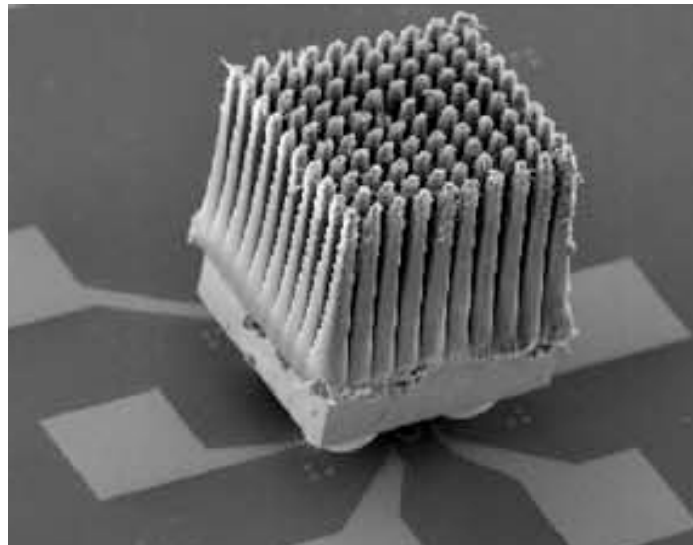
(b)

Figure 1.5 (a) Thermal conductivity of CNTs compared with the best thermally conducting materials, (b) SEM image of fine structure constructed from a uniformly aligned array of MWNTs reprinted with permission [9].

CNT-based AFM Tips

AFM probes are usually made of micro machined silicon cantilevers with integrated pyramidal tips. Such tips have a typical radius of about 10 nm. CNT-based supertips with superior characteristics (stability, resolution, lifetime, mechanical strength) can overcome the limitations of micro-machined silicon tips.
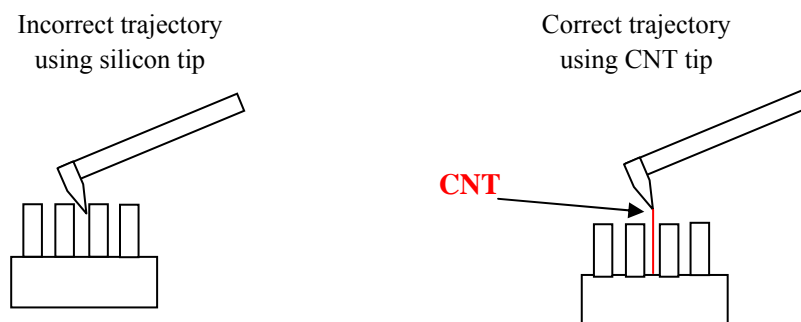
Figure 1.6 Comparison of AFM tips (without and with CNT).

Fuel Cell and Hydrogen Storage:

The strong capillarity of CNTs due to their tubular shape, together with their high surface/weight ratio, make CNTs ideal for gas adsorption, and hence for fuel cell and hydrogen storage applications [2]. For many applications, the availability of ensembles of CNTs with uniform diameters, length, and electronic properties is important, e.g. for electric leads, metallic CNTs are needed, but transistors require semiconducting tubes. To date there is no existing CNT synthesis method that sufficiently allows the control over length, diameter, or the electronic properties of the CNTs.

Chapter 2

CARBON NANOTUBES SYNTHESIS METHODS

Carbon nanotubes (CNTs) can be synthesized from a carbon source such as graphite (solid pure carbon source) or from a number of organic compounds (precursors) by their decomposition in an inert environment. In order to arrange carbon atoms to form a CNT, some source of energy is required. There are different methods to impart energy to carbon atom and to provide an environment so that they can bond together to form CNTs. The major methods presented in the literature are discussed below.

2.1 Arc Discharge Synthesis

The carbon arc discharge method, initially used to produce C_{60} fullerenes, is the first recognized method for the growth of both SWCNTs and MWCNTs [7]. In this method, two graphite rods (anode and cathode) are used as electrodes and He or Ar gas is introduced to produce an inert atmosphere. A low-voltage (~12 to 25 V) and high-current (50 to 120 amps) power supply is connected to the electrodes. As the rods are brought close together, an arc is produced across a 1-mm gap between two graphite electrodes 5 to 20 mm in diameter as shown in Fig. 2.1. The temperature rises to 3000 - 4000°C and evaporates carbon atoms from the anode; ionized carbon atoms are attracted to the graphite cathode and stick to it in the form of tube in addition to fullerenes and

amorphous carbon. The electric field in the plasma enables the growth of vertically aligned CNTs.

Iijima [3] discovered MWCNTs in 1991 in a sample prepared by this method. He found that nanotubes formed on the cathode, along with soot and fullerenes. Iijima and Bethune were the first to report on the production of SWCNTs [See ref. 7 and references therein].
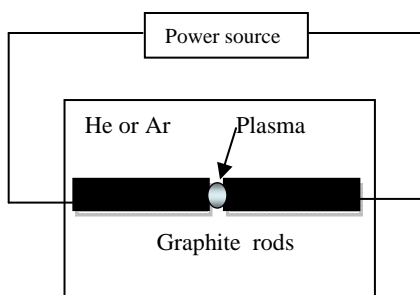
Figure 2.1 Schematic diagram of an arc discharge chamber.

Bethune [12] and Iijima [13] both found that SWCNTs could only be grown by adding metal catalyst to the anode. Iijima used an Fe:C anode in a C_4H_4:Ar environment, while Bethune used a Co:C anode in a He environment. A mixture of Ar:He gas is mostly used in the growth of CNTs. By tailoring the Ar:He gas ratio, the diameter of the SWCNTs formed can be controlled, with greater Ar content yielding smaller diameters[7]. The anode–cathode distance can be changed to vary the strength of the plasma formed in between. MWNTs can be obtained by controlling the pressure of inert gas in the discharge chamber and the arcing current. Ebbesen & Ajayan [14] synthesized MWCNTs on large scale using arc-discharge in 1992.

Shi *et al.* [15] produced cloth-like soot containing about 40% single wall carbon nanotubes (SWCNTs) with a Y–Ni alloy composite graphite rod as anode for D.C. arc-discharge. The SWCNTs had nearly the same diameter of 1.3 nm and were armchair (*n*, *n*) type carbon nanotubes (*n*=8, 9, 10 and 11). Ando *et al.* [16] have used an arc jet method, a modified form of arc discharge, to increase the ratio of SWCNTs in soot. They used Fe with graphite to grow SWCNTs.

The large amount of energy consumption makes this process less favorable for CNT production. Achieving stable discharge plasma is another factor in generating an environment favorable to CNT growth. As the anode is consumed, it has to be moved towards the cathode continuously. The stability of an electric arc is limited due to its moving nature on the cathode and anode surface. The nanotubes produced by this method need a lot of purification before use [2,7].

2.2 Laser Ablation Synthesis

In this process, a carbon target containing Ni and Co is placed in a tube furnace heated to 1200°C and intense laser pulses are used to ablate the target under inert atmosphere; a schematic setup is shown in Fig. 2.2. Nanometer-size metal catalyst particles are formed in the vaporized graphite. The metal particles catalyze the growth of SWCNTs but many by-products are also formed at the same time. The carrier gas-flow sweeps most of the carbon species produced by the laser evaporation out of the furnace zone depositing it as soot on a water-cooled copper rod.
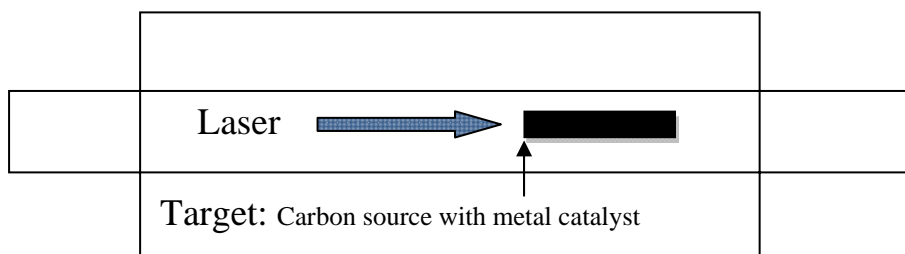
Figure 2.2 Schematic diagram of a laser ablation furnace.

The produced SWNTs are mostly in the form of ropes consisting of tens of individual carbon nanotubes [7, 11]. The yield varies from 20 to 80% of SWCNTs by weight. The by-products of this synthesis are graphitic and amorphous carbon, "Bucky onions" (concentric fulleroid spheres) surrounding metal catalyst particles and small fullerenes (C_{60}, C_{70}, etc.). When pure graphite is used MWCNT are produced. For very pure material with a narrow diameter distribution the laser ablation method is the process of choice [11].

2.3 Chemical Vapour Deposition (CVD)

Chemical vapour deposition (CVD) is the catalytic decomposition of hydrocarbons or carbon precursors with the aid of supported transition metal catalysts. The CVD method is the most suitable carbon nanotube synthesis method in terms of product purity and large scale production [17]. A variation of CVD, Plasma Enhanced CVD (PECVD), is an alternate solution being tested by some researchers [18]. In the synthesis of CNTs (single- or multi-walled) by CVD, thermal energy is imparted to hydrocarbons to break them into reactive radical species in the presence of catalyst like

Co, Ni, or Fe. CVD temperatures vary between 600 and 1200°C. Fig. 2.3 shows the schematic diagram of the CVD technique. The transition metal sources vaporize at temperatures much lower than that for the gas phase pyrolysis of the carbon sources. For example, ferrocene or $Fe(CO)_5$ evaporates at 200°C. The iron particles condense together and form clusters. An iron cluster of 40 to 50 atoms (~0.7 nm diameter) is about the size of the smallest SWNT. Smaller clusters tend to evaporate and are unstable. Very large clusters are also not ideal for nanotube growth because they favor graphitic overcoating. Declustering or breakup of large clusters also happens in the reactor. It is the competition between various processes (clustering and evaporation) that creates favorable size clusters. By tuning of various parameters such as temperature, flow rates of various carrier gases, injection velocity of the $Fe((CO)_5)_2$, residence time, etc., it is possible to obtain reasonable quantities of nanotubes. The kinetics of cluster formation and nanotube growth reactions is not well understood [see ref. 2, 7 and references therein].
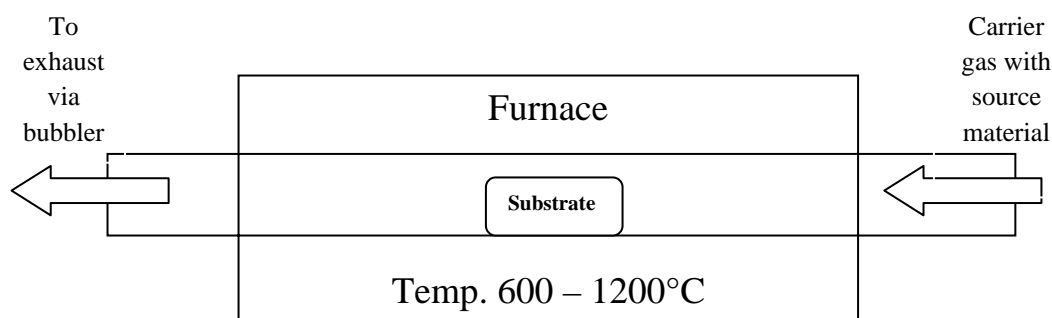
Figure 2.3 Schematic diagram of the CVD technique.

CNTs growth in CVD can be split into two basic types depending on the location of the catalyst, gas phase growth or floating catalyst and substrate growth. In gas phase

growth, the catalyst formation and nanotube growth occur literally in mid-air. In substrate growth, catalyst nanoparticles or metal precursors are deposited on a substrate such as SiO_2. In substrate growth, once the nanotube begins to grow by either surface or bulk carbon diffusion, the CNT will undergo either base growth or tip growth (Fig. 2.4). In base growth the catalyst particle remains attached to the surface and the nanotube is extruded into the air or along the surface. During tip growth, the end of the nanotube remains stuck to the surface and the catalyst particle shoots into the air at the opposite end of the extruding nanotube. Tip growth is considered the dominant mechanism for MWCNT growth, and base growth is dominant for SWCNT growth [7].

The generally accepted model for carbon nanotube growth proposed by several researchers is shown in Fig. 2.4. Metal particles are supported on the substrate material and either strong or weak metal– substrate interaction is assumed. High activity of carbon in the gas phase drives itself to dissolve in the nano-sized catalyst particles (transition metals: Ni, Co, or Fe). The particles may thus easily become supersaturated or saturated with carbon atoms arising from the decomposition of hydrocarbon gases.

(a) Bottom growth   (b) Top growth
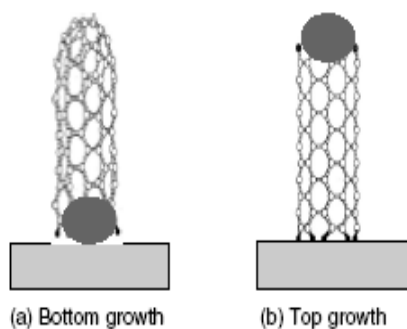
Figure 2.4 Schematic diagram of bottom (or base) growth and tip growth of nanotubes on a substrate, reprinted with permission [11].

The precipitation of carbon from the saturated metal particles leads to the formation of tubular carbon solids in sp^2 structure. In Fig. 2.4a, carbon nanotubes grow upward from the metal particles that remain attached to the substrate because of strong metal–substrate interaction (base growth mechanism). In the case of weak metal–substrate interaction (Fig. 2.4b), the particles are detached from the substrate and move up to the head of the nanotubes (tip growth mechanism).

Once a nanotube begins to grow, the diameter is set and will not change as growth continues. At the onset of growth, the catalyst particle and the resultant nanotube are of similar size, which means that one particle leads to only one nanotube during a single growth step. There are cases in which long nanotubes have been shown to change chirality along their length, which is due to some structural defect induced during the growth. For a catalyst particle of unchanging size, the growth of CNTs should continue until the hydrocarbon is shut off, either by removing the feedstock from the reaction area or by amorphous or graphitic carbon fully coating the particle [7].

2.3.1 Substrate Choice and its Effects

In CVD method CNT growth temperature lies in the range of 500 – 1200 °C, so the substrate material should have a melting point well above the growth temperature. Different substrate materials reported in the literature and their effect on the CNT growth are discussed here. Ortega-Cervantes *et al*. [19] synthesized carbon nanotubes on different substrate materials like: quartz, conductive glass, porous alumina and nickel

plates, using Fe and Co catalysts and ethanol as the carbon source. Successive nanotube growths were achieved on conducting glass, nickel plates and porous alumina substrates. Nickel plate and porous alumina substrates revealed SWNTs, whereas conducting glass substrate revealed MWNTs [19]. Biao Wang *et al*. [20] studied the growth of CNTs on various metal and metal coated substrates and found that good quality uniform CNTs were grown on Ni, Ti, Ta and Al coated (~100nm thick layer) Si wafer but no CNTs were grown on Cu, Au and Si wafer coated with Ni-Cr. Cinar Oncel and Yuda Yurum [21] reported in their review the use of Si, SiO_2, Ni, AIOP-5, Al_2O_3, Graphite fibers, MgO and $CaCO_3$ as substrates by different researchers and cited corresponding references. Kumar *et a.l* [22] have used the quartz tube of the CVD system itself as a substrate and collected the CNTs grown on the inner wall of the tube, from camphor and ferrocene. Wei *et a.l* [23] have used quartz and spheres of ZrO_2 as substrates and found that CNTs growth on ZrO_2 was more efficient. Liu *et al.* [24] used a flat sheet of graphite with predeposited layers of Al and Fe on it and have successfully grown VACNTs with water assisted CVD. Baddour *et a.l* [25] have used stainless steel in the form of plate, grid and powder and have grown a dense layer of CNTs without adding an additional catalyst.

2.3.2 Carbon Precursor and other Factors

The precursor for carbon nanotubes is fed into the system in the gaseous state at some specific conditions. To avoid oxidation of the carbon, the chamber is kept free of oxygen during the production process and a continuous inert gas flow is supplied to the

reaction chamber. Helium, Nitrogen and Argon are the most extensively used inert gases. Widely used carbon precursors are acetylene, methane, ethanol, ethylene, and toluene. Reaction time and gas flow rates, substrate temperature, catalyst type, carbon source and inert gas are important factors that affect the CNTs synthesis and product quality [19]. Porro *et al*. [26] used Si substrate and a mixture of camphor and ferrocene, as carbon source and Fe catalyst source, Nitrogen as a carrier gas and studied the effects of growth temperature, gas flow, substrate tilt angle and catalyst concentration. They used a Tagushi Matrix design approach [26] to optimize the deposition parameters and reported that CNTs with better physical and structural characteristics were obtained at a growth temperature of 800°C, 420ml/min carrier gas flow, 3.3% catalyst concentration and horizontal position of substrate. It is reported that lower synthesis temperatures than optimum synthesis temperature result in lower carbon nanotube yield in the product [27]. It is also reported that the reaction temperature plays an important role in the alignment properties and diameter of the synthesized nanotubes [28].

Usually, the carbon nanotube growth temperature (or reaction temperature) is between 550°C and 1200°C, and may vary according to the type of catalyst and support material used. Zhu *et al*. synthesized carbon nanotubes on graphite fibers by thermal CVD and showed that carbon nanotubes can only be grown in a limited temperature range. At low growth temperatures, only a carbon layer is formed on the fiber surface. However, at high temperatures, the diffusion rate of iron particles into carbon fibers was enhanced and the nanotube growth possibility reduced.

The flow rate of the carbon source gas is generally between 10 and 30 ml per minute. S. Musso [29] carried out the fluid dynamics analysis of gas flow in thermal CVD system designed to grow CNTs from Camphor and Ferrocene and reported the development of secondary transversal vortex flows caused by the effects of a temperature gradient inside the deposition system. They correlated the production of porous carbonaceous crust rich in iron particles on the top of very thick CNT mats to the irregular co-evaporation of the two reagents correlated with the difference of vapor pressure of camphor and ferrocene.

R. Brukh and S. Mitra [30] have studied the mechanics of CNTs growth by CVD from C_2H_4 and found that the optimum resident time of carbon source (C_2H_4) in the reaction zone is 0.5s. C_2H_4 decomposed to form elemental carbon via a sequence of free radical reactions, which then assembled as CNTs. The rate of carbon consumption leading to molecular growth increased with residence time. The residence time of the carbon source in the reaction zone depends on the carrier gas flow rate. Different carrier gases at the same flow rate have different effect due to the difference in their atomic/molecular weight [31]. Kumar *et al.* [22] reported that at high Ar flow (~100ml/min) most of the camphor-ferrocene vapour blow out of the reaction tube unpyrolyzed, resulting in low yield of CNTs. They propose a flow rate of 50ml/min or less for camphor-ferrocene mixture for good yield of CNTs.

Cinar Oncel and Yuda Yurum [21] reported in their review the catalytic activity of Fe, Co and Ni supported alumina and silica and reported that Fe and Co at 700°C give MWCNTs. They also reported that Fe resulted in the best crystallinity of the nanotubes

among Fe, Co and Ni catalysts. C. Du and N. Pan investigated the growth of carbon nanotubes directly on nickel substrate. They studied nucleation and growth behavior of nanotubes with respect to growth sites and reaction temperature and reported that; at lower synthesis temperatures nickel nanoparticles serves as the nucleation sites, however at high temperatures grain boundaries and defective sites are the nucleation sites. Also, a small amounts of iron nanoparticle deposition on nickel substrate results in an improvement of density of the carbon nanotubes.

There are also studies on the performance of the non-metallic catalysts. Cho *et al*. synthesized carbon nanotubes using dispersed magnetic fluids, instead of conventional metallic catalyst particles. Application of magnetic fluid of surfactant-coated magnetite nanoparticles by spin coating method on Si substrates resulted in successful growth of dense and aligned carbon nanotubes. Botti *et al*. reported carbon nanotube synthesis without metal catalyst addition. They fabricated carbon nanotubes and nanowires using amorphous hydrogenated carbon nanoparticles as precursor. It is demonstrated that the structure of the nanotubes obtained strongly depends on the catalytic particle size and chemical composition. Widely used catalyst materials in carbon nanotube synthesis are cobalt, iron, titanium, cobalt and nickel [see ref. 21 and references therein].

2.4 Summary

Carbon nanotubes (CNTs) are one of the most attractive materials for nanoelectronic, for reinforcing the material in composites and for applications as sensors, actuators and field emission devices. Intensive research activities to improve the synthesis methods and conditions, quality and productivity of the carbon nanotubes have been done in last two decades. However, the production of carbon nanotubes in a controlled way, in large amounts, and with well-defined properties has not yet been achieved. There are number of growth methods reported in the literature but the three most widely used methods for CNT growth are Arc Discharge, Laser Ablation and Chemical Vapor Deposition (CVD). The CVD method is believed to be the most suitable carbon nanotube synthesis method in terms of product purity, large-scale production and low-cost mass production technique of carbon nanotubes.

CVD is the catalytic decomposition of hydrocarbons or carbon precursors with the aid of transition metal catalyst. Most of carbon nanotube synthesis techniques require the introduction of catalyst in the form of gas particulates or as a solid support. The selection of a metallic catalyst affects the growth and morphology of the nanotubes. Widely used catalyst materials in carbon nanotube synthesis are cobalt, iron, titanium, nickel and combinations of these metals and/or oxides. Iron is considered as the best catalyst for small diameter CNTs. Most widely used carbon precursors are acetylene, methane, ethanol, 2-propanol, ethylene, toluene and camphor. The most common used carrier gases are He, N_2 and Ar. Flow rate of the carrier gas as well as carbon precursor in

gaseous form also affects the growth and quality of CNTs. Type of the substrate, growth temperature and deposition time also affect the growth and quality of CNTs.

In the present work camphor was used as carbon source, ferrocene as the source of Fe floating catalyst, Ar as carrier gas and Si and Quartz as substrates. The effects of three parameters (growth temperature, carrier gas flow and catalyst concentration) were studied in this research work in order to have better control over the economical and energy efficient growth of CNTs. A simple and economical CVD system was setup for the growth of CNTs. The parameters were optimized to achieve the lowest possible temperature for the growth of good quality CNTs. The lower the growth temperature the lower the energy consumption will be. It will also help the growth of CNTs on low cost substrates which will help reduce the production cost.

Chapter 3

CHARACTERIZATION OF CARBON NANOTUBES

There are many potential applications for Carbon nanotubes (CNTs), thanks to the nanometer dimensions and the remarkable physical properties. In order to comprehend their basic physical and chemical properties, a complete and correct characterization of carbon nanotubes is crucial. There are many techniques that are available to characterize carbon nanotubes, like Fourier Transform Infrared (FTIR) and Raman spectroscopy, Thermo-gravimetric Analysis (TGA) and electron microscopy (SEM, TEM). These techniques and the relevant information that can be obtained for CNTs are discussed in this chapter.

3.1 Infrared (IR) Spectroscopy

Spectroscopy is the study of the interaction of electromagnetic radiation with a substance. The nature of the interaction depends upon the properties of the substance. The electromagnetic spectrum covers a very wide range of frequencies or wavelengths. When electromagnetic radiation passes through a sample (solid, liquid or gas), certain frequencies of the radiation are absorbed by the molecules of the substance leading to the molecular excitations (vibrational or rotational or stretch or bending). The frequency of absorbed radiation is unique for each molecule, thus providing information on the characteristics of a substance. A molecule exposed to infrared radiation will absorb the radiant energy only if it matches the energy of vibration of that molecule. IR spectroscopy is a non-destructive, quick and relatively cheap spectroscopic technique.

There are seven to nine infrared active modes in SWCNTs, depending on the symmetry: chiral, zigzag and armchair [9]. Comparing the predictions for IR spectra of SWCNT for different symmetries, it is found that phonon modes around 850 cm^{-1} and 1590 cm^{-1} appear in all symmetries almost independently of the diameter and are therefore expected to produce clearly recognizable structures in absorbance or reflectance spectra of a variety of SWCNT. According to the theoretical model based on force-constants, the frequencies for small-diameter SWCNT are lower than the corresponding modes in a two-dimensional graphite layer and converge to the position of the graphite modes with increasing diameter [see ref. 31 and references therein]. Infrared (IR) spectroscopy is used to investigate the growth and purity of CNTs. It is often used to determine impurities remaining from synthesis or molecules capped on the nanotube surface. The Infrared spectrum exhibits all the modification of the CNTs structure and reveals the nature of compounds added to them. IR spectroscopy provides less information about the vibrational properties of carbon nanotubes because of the strong absorption of SWCNTs in the IR range. In transmission IR study of CNTs two features are present, i.e. a weak line at ~868 cm^{-1} and a broad asymmetric band at ~1575 cm^{-1}[36].

3.2 Raman Spectroscopy

Raman spectroscopy is based on the inelastic scattering of light by a material which produces a shift in wavelength of the incident light. It is one of the most useful and powerful techniques to characterize carbon nanotube samples. It does not require sample preparation, is a fast and non-destructive analysis technique. It allows for the detection and the study of a single and isolated CNT. This shift in wavelength is used to deduce

information about the material. Most light passing through a transparent substance undergoes elastic scattering, called Rayleigh scattering. In Rayleigh scattering a photon interacts with a molecule, polarizing the electron cloud and raising it to a "virtual" energy state. This is extremely short lived (on the order of 10^{-14} seconds) and the molecule soon drops back down to its ground state by releasing a photon. Since the molecule is dropping back to the same state it started in, the energy released in the photon must be the same as the energy from the initial photon. Therefore the scattered light has the same wavelength.

In Raman scattering the light photons lose or gain energy during the scattering process. If the molecule is promoted from a ground to a virtual state and then drops back down to a (higher energy) vibrational state then the scattered photon has less energy than the incident photon, this is called Stokes scattering. If the molecule was already in a vibrational state and after scattering of the incident photon it goes to its ground state then the scattered photon has more energy, this is called anti-Stokes scattering.
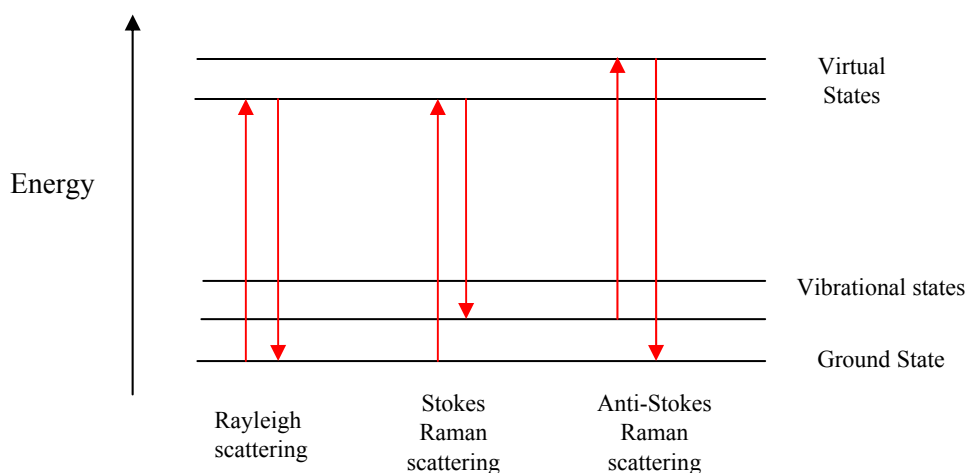
Figure 3.1 Three different forms of scattering of electromagnetic radiations from matter.

Only about 1 in 10^7 photons undergo Stokes Raman scattering. The amount of anti-Stokes scattering is even less than Stokes scattering. Normally in Raman spectroscopy only the Stokes half of the spectrum is used, due to its greater intensity [32].

3.2.1 Raman Spectroscopy of CNTs

A CNT consists of a graphene sheet rolled in a tube, vibrational modes of CNT are derived from those of graphene by applying boundary conditions along the circumference [36]. The first paper on Raman scattering in single wall carbon nanotubes (SWCNTs) was published in 1997 by Rao *et al.* [33]. A typical Raman spectrum is shown in Figure 3.2. Raman spectrum of CNTs can be divided into three main parts, the radial breathing mode (RBM), the disorder induces mode (D mode) and the high-energy mode (HEM). Each part is used to access different properties of single-walled carbon nanotubes. There are two dominant Raman signatures of CNTs in these Raman spectra that distinguish a SWCNT from other forms of carbon. First, the low-frequency feature, usually in the range 100-300 cm^{-1}, is arising from scattering by the radial breathing modes (RBM) which correspond to symmetric in-phase displacements of all the carbon atoms in the SWCNT in the radial direction. Second, the double-peak structure (around 1500-1600 cm^{-1}) is associated with the tangential (G band) vibrational modes of SWCNTs and is related to the Raman-allowed feature appearing in Raman spectra for graphite [5]. Neither the RBM feature nor the multi-component G band features are observed in any other sp^2 bonded carbon material.
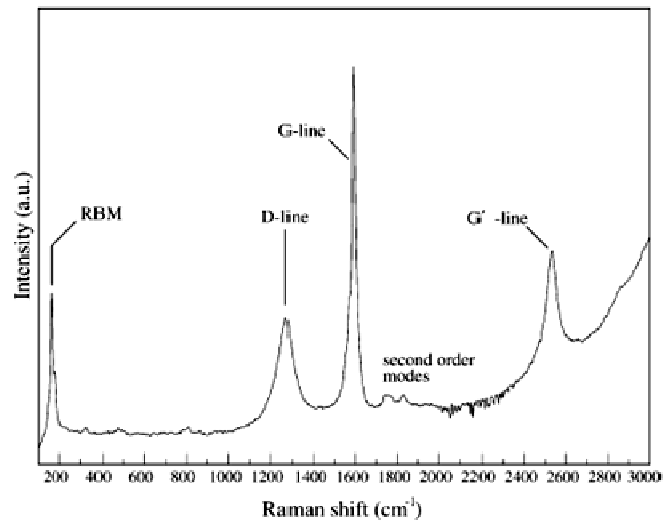
Figure 3.2 Raman spectrum showing the most characteristic features of CNTs:
radial breathing mode (RBM), the D band, G band and G´ band, reprinted with
permission [5].

Typically, sp^2 bonded carbon materials show a characteristic single G band (Lorentzian
shape) Raman peak at about 1582 cm^{-1}. These two first-order Raman features (the RBM
and the multi G-band) are the spectral signatures of SWCNTs and have been used to
characterize nanotube samples from their earliest stage of identification [8]. The RBM
from MWCNTs is only observed when they have very small diameter inner tubes (below
3 nm). The *G* band in MWCNT is both small in intensity and smeared out due to the
effect of the diameter distribution within the individual MWCNT, and because of the
variation between different tubes in an ensemble of MWCNT in typical experimental
samples [40].

The line shape for the lower frequency G-band feature for metallic (M) tubes is
broader, following a Breit-Wigner-Fano line shape [39], and is downshifted in frequency
from semiconducting (S) tubes of similar diameter. The spectra taken for different laser

excitation energies differ from one another due to the resonance Raman Effect. Each (n, m) nanotube has a different set of electronic resonance levels, so that each laser line accesses a different set of nanotubes. Since the number of atoms around the circumference of a tube is proportional to the nanotube diameter, it is expected that the frequency of the RBM mode ω_{RBM} will depend on the inverse tube diameter, as observed experimentally [7, 8,31].

3.3 Thermogravimetric Analysis (TGA)

Thermogravimetric analysis (TGA) is an analytical technique used to determine a material's thermal stability and its fraction of volatile components by monitoring the weight change that occurs as a specimen is heated. The measurement is normally carried out in air or in an inert atmosphere, such as Helium or Argon, and the weight is recorded as a function of increasing temperature. In addition to weight changes, some instruments also record the temperature difference between the specimen and one or more reference pans (differential thermal analysis, or DTA) or the heat flow into the specimen pan compared to that of the reference pan (differential scanning calorimetry, or DSC). DSC can be used to monitor the energy released or absorbed via chemical reactions during the heating process.

3.3.1 Thermogravimetric Analysis (TGA) of CNTs

In case of the carbon nanotubes, TGA analysis is performed in an oxidative atmosphere (air or oxygen) with a linear temperature ramp. The maximum temperature is selected so that the specimen weight is stable at the end of the experiment, implying that

all chemical reactions are completed (i.e., all of the carbon is burnt off leaving behind metal oxides). The weight change in an air atmosphere is a superposition of the weight loss due to oxidation of carbon into gaseous carbon dioxide and the weight gain due to oxidation of residual metal catalyst into solid oxides [34]. The following information can be obtained from TGA.

i.   Residual mass (M_{res}): the ash content or the mass of residual metal oxide,

ii.   Oxidation temperature (T_o): the temperature of the maximum in the weight loss rate (dm/dT_{max}) and

iii.   The weight loss onset temperature (T_{onset}): the temperature when oxidation just begins.

Gradual onset is believed to be due to nanotubes being contaminated with amorphous carbon and other types of carbonaceous impurities that oxidize at temperatures (~400°C) lower than that of nanotubes. Weight loss due to carbon oxidation is often superimposed on the weight increase due to catalyst oxidation at low temperatures and in some cases this leads to an upward swing of the TGA curve prior to the bulk of the weight loss. TGA measurement of "as-produced" nanotube material in air usually produces only one peak in the dm/dT curve, as "fluffy" raw nanotubes oxidize rapidly in an oxygen-rich environment. The oxidation temperature T_0 provides a measure of the thermal stability of nanotubes in air and it depends on a number of parameters like diameter of the tube (smaller diameter nanotubes are believed to oxidize at lower temperature due to a higher curvature strain), defects in nanotube walls (can lower the thermal stability), metal particles present in the nanotube specimens (amount of metal impurity in the sample influences the thermal stability). Thermal stability is a good measure of the overall quality of a given nanotube sample. Higher oxidation temperature

is always associated with purer, less defective samples [35]. A large spike in the temperature difference (DTA) plot (temperature goes up by 10-20 $^{\circ}$C, and then comes down and continues along a linear ramp) is a signs of combustion (i.e., the sample starts burning and releases a considerable amount of heat very quickly, causing a sharp increase in temperature followed by heat dissipation and a subsequent temperature drop). This behavior is more often observed on as-produced unpurified nanotubes that are "fluffy" and have more metal catalyst. Typical heating rates employed in TGA measurements of carbon nanotube specimens are in the 5-20 °C/min range.

3.4 Electron Microscopy

Electron Microscopes use a beam of highly energetic electrons to examine objects on a very fine scale. Electron microscopy techniques enable us to see and study carbon nanotube structures in great detail. The instrument development was driven primarily by the well-known limitations of the light microscope. In electron microscopy a beam of energetic electrons is incident on the sample. As a result of interaction of this beam different types of electrons and radiations are emitted from the sample and the substrate which are detected and used to construct the image of the sample. There are two well known types of electron microscopes: scanning electron microscope (SEM) and transmission electron microscopes (TEM).

3.5.1 Scanning Electron Microscopy

In order to observe nano size objects like CNTs, the use of an SEM is necessary to overcome the limited angular resolution of optical microscopes [38]. Both nanotube powder samples as well as individual tubes on a bulk substrate (e.g., silicon wafer) can be observed by SEM. A fine electron probe is scanned across the sample surface while recording the current of the electrons emitted from the sample surface (called secondary electrons) due to interactions of incident high energy electron beam with the sample surface. The image is the intensity of the emitted electron current versus beam location at the sample. An image can be formed by the secondary electrons emitted from the sample surface as well as by the backscattered primary electrons.
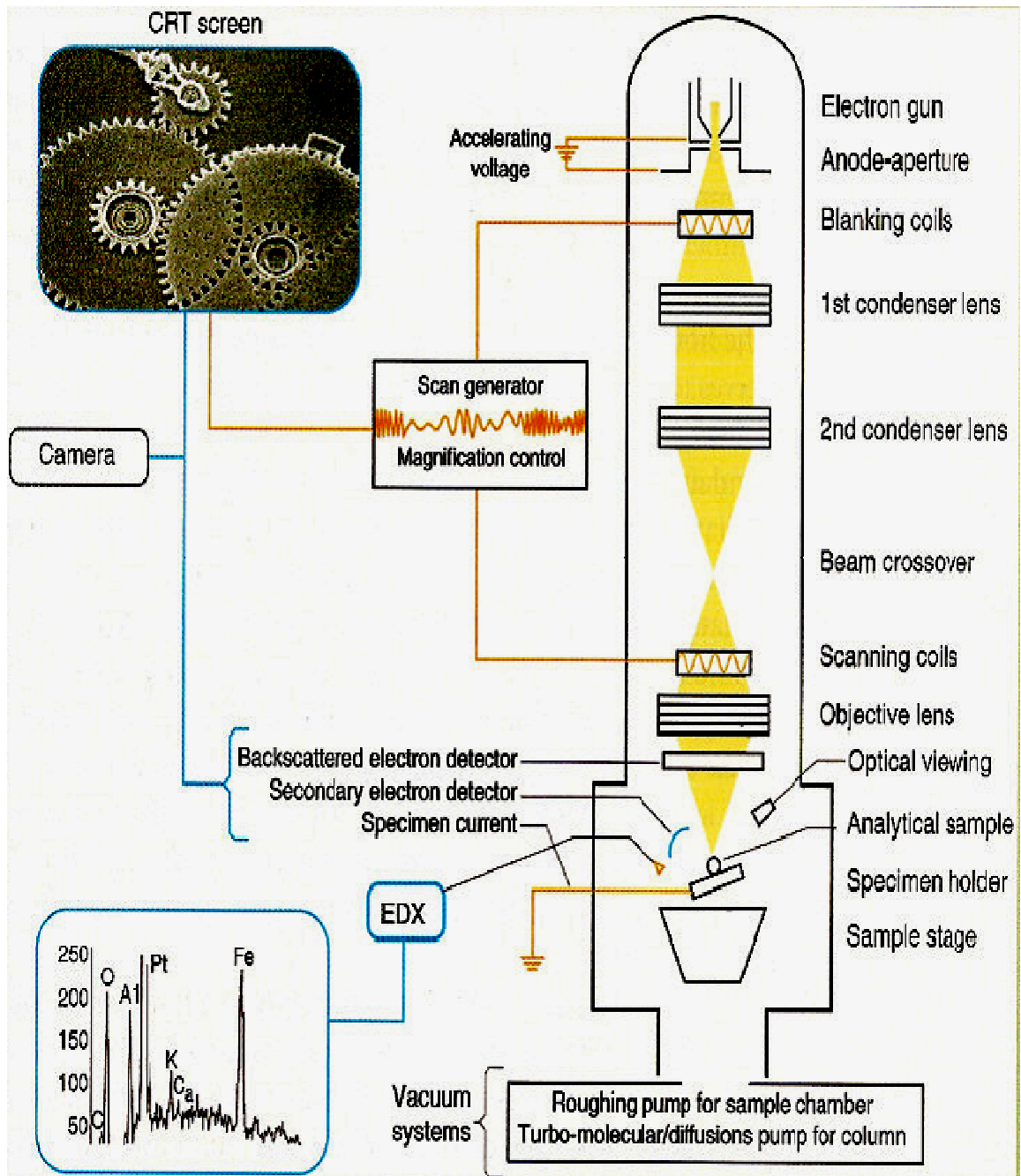
Figure 3.3 Schematic of SEM, reprinted with permission [4].

3.5.2 Transmission Electron Microscopy

Although SEM can be useful in imaging the tubular one-dimensional (1-D) structure of the MWCNTs, there is another method of electron microscopy that can be much more helpful in the structural studies of carbon nanotubes. This method is transmission electron microscopy (TEM), and it is a powerful technique that is used to determine the number of walls in a MWCNT [2,3] or image the isolated SWCNTs. It allows for the measurement of the tube diameters as well as investigation of structural defects in carbon nanotubes.

In fact carbon nanotubes (CNTs) were discovered using TEM when observing carbon soot produced in an electric arc between graphite electrodes. In a transmission electron microscope, the electron wave mainly experiences two basic processes during its propagation from the specimen to the image: interaction with the specimen and modulation by the electron-optical lens system. During the first process, the electron wave picks up the structure information of the specimen. In the second process, the structure information is transferred to the microscope. Due to the unique design of the TEM, the electron wave carrying the structure information forms an electron-diffraction pattern (EDP) on the back focal plane of the objective lens and an image on the imaging plane. Therefore, the EDP and the image can be simultaneously observed in the TEM. By using an aperture at the back focal plane of the objective lens to select the transmitted electron beam for imaging, a bright-field (BF) image is formed. A dark-field (DF) image is created by using one of the diffracted beams in the EDP for imaging. If a large aperture

is selected to allow both the transmitted electron beam and a set of diffracted beams to

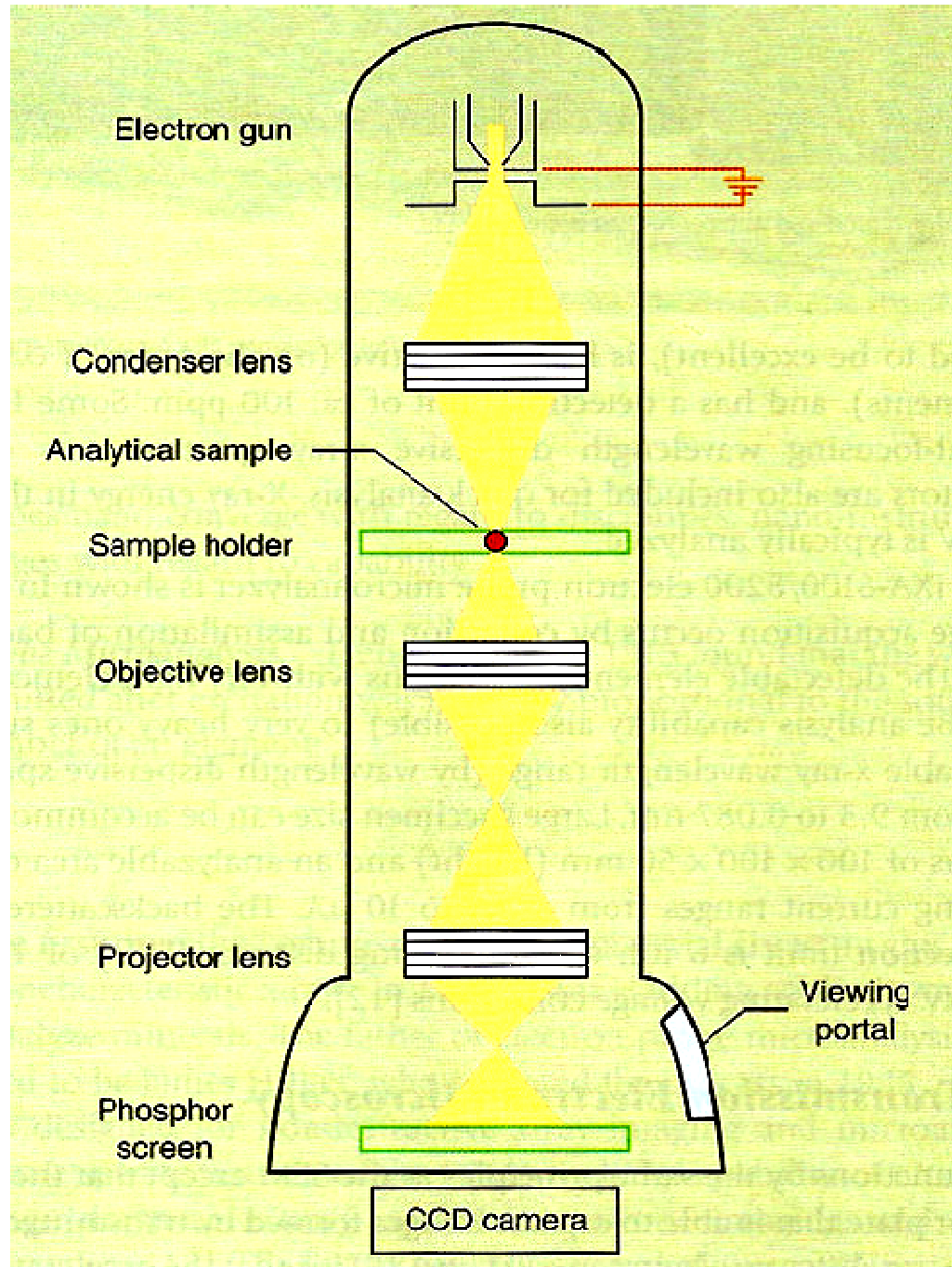pass through, a high-resolution TEM (HRTEM) image is formed.

Figure 3.4 Schematic of TEM, reprinted with permission [4]

Mainly due to the spherical aberration (Cs) of the objective lens in the microscope, the contrast of an HRTEM image is affected by the focusing conditions, and the image resolution is limited. As a result, a HRTEM image is usually not straightforward to interpret and it is hard to directly observe the atomic structure of carbon nanotubes (CNTs). Due to the recent development of the Cs-corrected HRTEM, the resolution of the microscope has dramatically improved to the sub-Å level. It is worth remembering that to minimize spherical aberration, the microscope is preferably operated at an acceleration voltage lower than 120 kV to minimize the knock-on atomic displacement damage of the CNTs by high-energy electrons, and to increase the image contrast.

TEM also has the option of the use of electron diffraction and electron energy loss spectroscopy (EELS) on the nano scale. Electron diffraction has been used to determine average helicity and the local variations of helicity of the individual SWCNT within the ropes of SWCNTs. Combined with x-ray energy dispersive spectroscopy, TEM has also enabled the identification of the catalyst composition responsible for nanotube nucleation [9].

3.5 Summary

There are a number of techniques for nanotubes characterization that are very useful for SWCNTs; however MWCNTs characterization needs more development. Infrared (IR) spectroscopy is used to determine impurities remaining from synthesis or molecules capped on the nanotube surface. TGA/DTA is used to find the product stability (by determining T_o- oxidation temperature) and impurities in the product. Due to small size of CNTs, Scanning Electron Microscopy (SEM) is an appropriate technique to be used for their characterization. Images taken by an SEM can be recorded almost in real-time. The geometric data of CNTs can be extracted from SEM images which can tell the type of CNTs (conductor or semiconductor) and the relatively huge vacuum chamber allows the analysis of large samples and provides enough space for robotic nano-manipulation systems for the handling and characterization of individual CNTs. Full characterization of MWCNTs like inter-shell spacing and internal diameter of the tubes cannot be done with SEM. TEM provides the ultimate resolution and helps in finding internal and external radii, inter-shell spacing of MWCNTs and objects inside CNTs. The most powerful technique to characterize nanotubes is the Raman spectroscopy: without sample preparation, a fast and non-destructive analysis is possible. RBM peaks in Raman spectra are used to find the diameter of SWCNTs and DWCNTs. Ratio of D and G peaks give the measure of the quality of CNTs. For a correct characterization of nanotubes, these techniques should complement each other.

Chapter 4

EXPERIMENTAL DETAILS

Carbon nanotubes can be grown from different carbon sources using different techniques as discussed in chapter 2. In the present work CNTs were grown by the chemical vapor deposition (CVD) method from a mixture of camphor and ferrocene. The experimental work discussed in this chapter consists of samples growth and their characterization. Samples growth process consists of: quartz tube cleaning, substrates cleaning and loading, samples growth in an inert atmosphere at pre-set temperature and cooling of furnace to room temperature. Three sets of samples were grown under different conditions. Details of these steps are given in the first part of this chapter. Sample characterization was performed by TGA, Raman and IR spectroscopy and electron microscopy (SEM and TEM) techniques. Details of characterization are given in the second part of this chapter.

4.1 Samples Growth

4.1.1 CVD Setup

The CVD setup used in the present work consists of a tube furnace (Barnstead Tube Furnace, Model F21100), a 115cm long quartz tube of 5 cm diameter, a heating coil, a flow meter(, an Ar gas cylinder and an oil bubbler arranged as shown in Fig. 4.1. The quartz tube is placed in the furnace in such a way that the left end of the tube is 45 cm away and the right end is 70 cm away, form the center of the furnace. This off centric position of the quartz tube was chosen in order to leave   room for the source material to be placed inside the tube away from the furnace. A separate setup

for the heating of the source material consists of a resistive heating wire wrapped around the tube near the right end of the tube (~15 cm from right end of the tube).
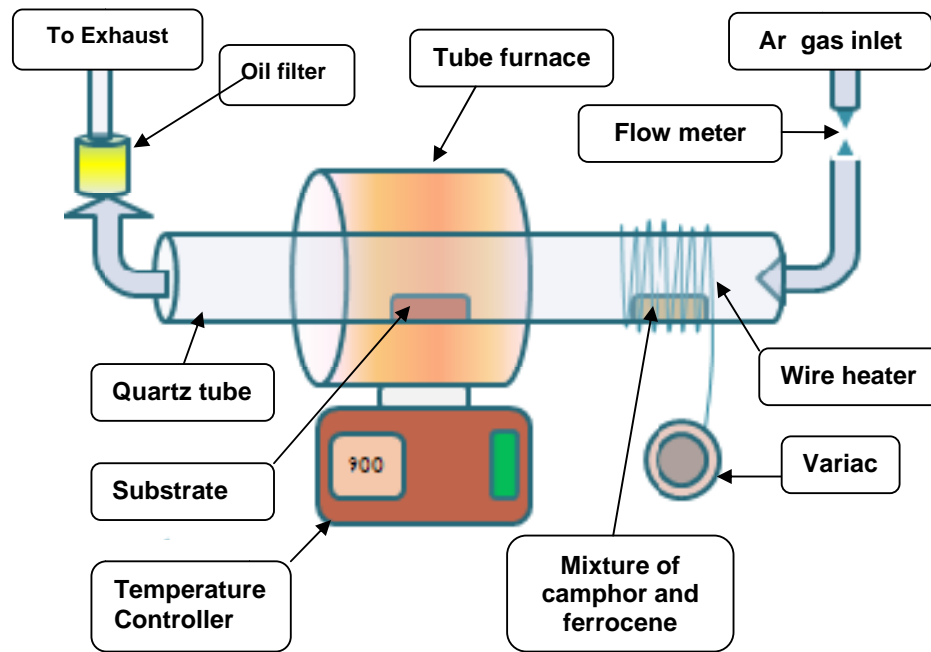
(a)
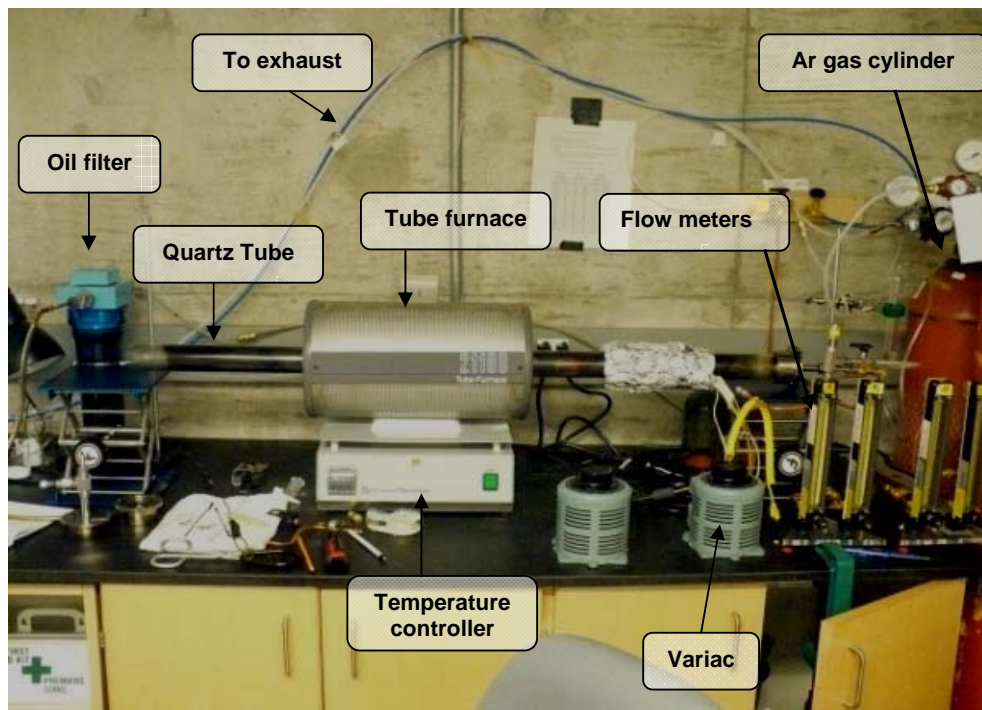
(b)

Figure 4.1 (a) Schematic of CVD setup, (b) Picture of CVD setup

The right end (inlet) of the tube is connected to the Ar gas tank through floating ball flow meters and the left end (outlet) is connected to the exhaust via the oil bubbler. The temperature of the furnace, i.e. the second zone, is controlled by a programmable microcontroller whereas the temperature of the first zone is controlled by the current to the heating coil, delivered with the help of a variac and measured with an IR probe connected to a digital temperature meter.

4.1.2 Quartz Tube Cleaning

The quartz tube was cleaned thermally at 900°C in an oxidative environment for 20 min with compressed air flown at 500sccm into the tube. The tube was then cooled down to room temperature before loading the substrates and source materials.

4.1.3 Substrate Choice

For CNTs to be used in electronics, they need to be grown on some support or substrate. One of the factors considered in the choice of the substrate is its thermal stability at high temperatures. As in CVD, the growth temperature may go up to 1200°C so the substrate material must have a melting point greater than the growth temperature. Different types of substrates are reported in the literature as discussed in chapter 2. In this work cSi and $cSiO_2$, i.e. quartz, were chosen as substrates so that the CNTs grown on them could be characterized by IR and UV-vis spectroscopy techniques respectively. Both have melting temperature well above the 1000°C which was the highest growth temperature used.

4.1.4 Substrate Cleaning

Substrate cleaning is crucial in order to get rid of contaminations like manufacturing and packaging residues, finger prints and oil and dust particles. Contamination can affect the growth process and also the properties and performance of the grown sample. Both cSi and cSiO$_2$ substrates were cleaned ultrasonically in acetone (CH$_3$COCH$_3$) for 5 minutes, then in methanol (CH$_3$OH) for 5 minutes, then in deionized water for 5 min, and finally were dried by blowing (compressed) air.

4.1.5 Samples Growth Procedure

Cleaned substrates were immediately placed on an alumina boat and loaded into an already cleaned quartz tube at the center of the heating zone in the furnace. Appropriate quantities of camphor and ferrocene (3~4 gm) were placed in an another alumina boat, which was positioned inside the quartz tube, nearly 30 cm on right side from the centre of the furnace and nearly 15cm left from the right end of the quartz tube, as shown in Fig. 4.1.

Three sets of samples (consisting of 21 samples in all) were prepared from a Camphor–Ferrocene mixture. Iron (Fe) from the decomposition of ferrocene served as catalyst. Carbon from ferrocene and camphor served as the carbon source. For the first set of samples the growth temperature was varied from 750 °C to 1000°C with a step of 50°C, at a constant carrier gas (Ar) flow rate of 50sccm and ferrocene to camphor ratio of 3.3 to 100. In the second set, the carrier gas (Ar) flow rate was changed from 10sccm to 50sccm in steps of 10sccm, and then two more samples were grown at 80sccm and 100sccm, at a constant growth temperature of 900 °C and

1000°C with a step of 50°C, at a constant carrier gas (Ar) flow rate of 50sccm and ferrocene to camphor ratio of 3.3 to 100. In the third set the catalyst concentration (ferrocene percentage in the mixture) was varied from 0 to 5% with a step of about 1% and the growth temperature was kept constant at 900°C with constant carrier gas (Ar) flow rate of 50sccm. Table 4.1 shows the different parameters for all samples. Although CNTs were clearly observed at all growths, the quality, quantity and position of the nanotubes deposited were found to be different in different growths.

Table 4.1

Detail of the samples grown at different pyrolysis temperatures.

Set-I Growth Temperature Variation (with catalyst concentration 3.3% and flow rate 50sccm)		
S.No.	Growth Temperature (°C)	Sample ID
1	750	CNT28-02-09
2	800	CNT05-02-09
3	850	CNT25-03-09
4	900	CNT18-02-09
5	950	CNT23-02-09
6	1000	CNT23-03-09
7	900	CNT31-03-09
8	900	CNT07-04-09

Table 4.2

Detail of the samples grown at different flow rates of carrier gas.

Set-II Carrier Gas (Ar) Flow rate Variation (with catalyst concentration 3.3% and growth temp. 900°C)		
S.No.	Carrier Gas Flow rate (sccm)	Sample ID
9	10	CNT09-05-09
10	20	CNT12-05-09
11	30	CNT13-05-09
12	40	CNT19-05-09
13	50	CNT31-03-09
14	80	CNT21-05-09
15	100	CNT20-05-09

Table 4.3

Detail of the samples grown with different catalyst concentrations

Set-III Catalyst Concentration Variation (with growth temperature 900°C and flow rate 50sccm)		
S.No.	Catalyst Concentration (%)	Sample ID
16	0	CNT05-05-09
17	1	CNT04-05-09
18	2	CNT01-05-09
19	3.3	CNT31-03-09
20	4	CNT06-05-09
21	5	CNT07-05-09

In the growth process, first, argon gas was passed at a rate of 500sccm for 30 minutes to expel atmospheric air out of the reaction tube, then the flow was reduced to 50sccm (or the other required flow rate) and the furnace was turned on with a set pyrolysis temperature (750–1000 °C). When the furnace reached the set temperature, the current to the heating element was turned on and slowly increased using a variac and the temperature was monitored with an IR probed digital temperature meter. The mixture of camphor and ferrocene was heated to ~200°C in the first region of the quartz tube. Vapors of camphor and ferrocene were carried out by Ar gas into the second region of the furnace where pyrolysis took place and CNTs were grown on the substrates and on the inside of the walls of the quartz tube. The material (CNTs or other products or unpyrolysed camphor or ferrocene) that did not deposit on the substrate or walls of the quartz tube, were collected via the oil bubbler attached at the outlet. The whole sample growth process took 5 to 15 minutes. When the source material exhausted, both the heating sources were turned off and the furnace was cooled down to the room temperature under Ar flow. Once the furnace was cooled down, samples were removed and the furnace was cleaned using the above mentioned method, for the next deposition.

4.1.6 An Interesting Observation

A dense bridge of CNTs/CNFs was observed between the Si and Quartz substrates nearly 3 mm apart. It "welded" the two substrates strongly so that when trying to move the quartz substrate from the holder, the Si substrate got dragged along with the quartz substrate. This is shown in the following picture. Further investigation of the mechanical strength of this "CNTs/CNFs Bridge" is to be done.
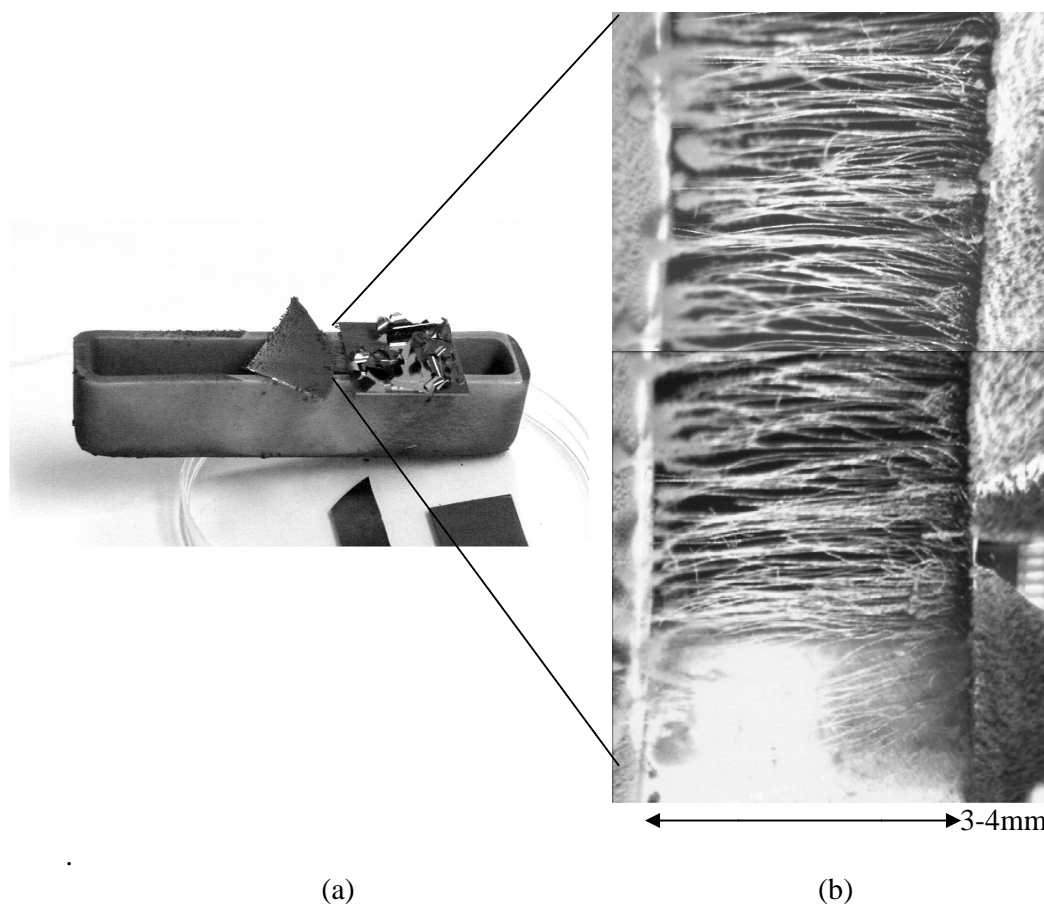

3-4mm

.   (a)   (b)

Figure 4.2 (a) Picture of the substrates on mica boat CNTs/CNFs Bridge,
(b) Magnified view of the bridge taken with an optical microscope.

4.2 Characterization

All the samples in the powder form were characterized by TGA, Raman and FTIR (using HATR) spectroscopy, and electron microscopy (SEM/TEM) techniques. These techniques and the instruments involved are discussed in the following sections of this chapter and the results are presented in chapter 5.

4.2.1 Thermogravimetric Analysis (TGA)

TGA analysis were done using a Q Series SDT Q600 Model (TA Instruments) in air with flow rate of 50mL/min. The temperature range was chosen from 30 ℃ to 1000 ℃ with a ramp rate of 5℃/min. No sample preparation was required for TGA. Masses between 5mg and 12 mg of as collected CNTs powder scratched from the quartz tube were filled in a small alumina boat and loaded into the heating compartment of the instrument. Data was collected at the rate of 1 point per second.

4.2.2 Raman Spectroscopy

Raman spectra were acquired with a Renishaw inVia Raman Microscope RE 02, at Trent University, in Peterborough ON. The instrument used a He-Ne laser with 633nm wavelength, 50 mW (max. power) and a spot size ~5µm. No sample preparation was required: a small spec of CNTs powder was placed on a glass slide under the objective lens of microscope. The microscope was focused and the spectra were collected with the following settings:

Accumulation time: 90sec,

Number of scans (accumulations): 5

and Objective lens setting: X20

4.2.3 IR Spectroscopy

FTIR spectra were taken using a Perkin Elmer Spectrum 100 with HATR accessory. A sample in the powder form was spread over the ZnSe crystal of the spectrometer and pressed with the force arm attached to the instrument. Spectra were collected in the wavenumber range $400cm^{-1}$ to $4000cm^{-1}$ with a resolution of $4cm^{-1}$ and 10 accumulations.

4.2.4 Electron Microscopy

A small quantity of CNT powder was dispersed in methanol using a sonicator, for 3-5 minutes to make a very dilute (nearly clear) solution. A drop from this CNT-methanol solution, was placed on TEM grid (carbon coated copper mesh) with the help of a pipette and the grid was left to dry under a table light lamp (at temperature ~ 40 - 50°C) for nearly 15 minutes. Then the dried grid was placed (loaded) into a JEOL 2010F transmission electron microscopy, to acquire TEM micrographs. Upon the completion of TEM analysis the grid was removed (unloaded) and used in a JEOL 7000F scanning electron microscope. SEM micrographs were obtained at different magnifications and accelerating voltages.

4.3 Sources of error and possible improvements in the present CVD setup

1. *Blockage of outgoing pipe/connector*: The mixture of ferrocene and camphor boils off very quickly around 160°C and the vapors of the mixture flood out of the quartz tube passing through pyrolysis zone and condense on the inner side of the metallic connector and affect the gas flow. Sometimes the tube is blocked

completely and the gas flow stopped, which affected the CNTs growth process and hence the product quality. If the pressure buildup inside the tube is too high then it will flow back through the safety valve (connected with inlet of the quartz tube) and there is a chance of blockage of the overflow pipe as well. So the coupler used to connect the quartz tube with the oil bubbler (outlet) can be changed with one having a bigger diameter of the extending pipe.

2. *Control of temperature of mixture heating zone (zone one)*: Catalyst and precursor mixture is heated in the first zone of quartz tube using a wire element wrapped around the tube and current flow to the heating wire is controlled with the help of a variac. With the present setup it is not possible to control the ramp rate of temperature and to set a specific temperature limit. If this zone is equipped with a temperature controller then this problem can be fixed. It was observed during present deposition work that a low temperature ramp (by increasing current in small steps) helps in preventing a quick boiling of the mixture and decreasing the chances of the blockage of the tube.

3. In the mixture of camphor and ferrocene the boiling point of camphor is less than that of ferrocene so camphor evaporates before the ferrocene which is undesired. This problem could be solved by splitting the first heating zone into two zones with different temperature controllers.

4. Precise positioning (individual and relative to each other) and the orientation of the substrates and source materials in both heating zones can help in the reliability and repeatability of the sample growth.

Chapter 5

RESULTS AND DISCUSSION

Three sets of samples were grown under different growth conditions. CNTs were clearly observed under all growth conditions, however the quality, quantity and position of the nanotubes grown were found to be different for different growth parameters.

A thin film of carbon with small hair-like structures on substrates surfaces and edges, a hair-like bridge between neighboring substrates, a thick mat of CNTs and other carbon products on the inner wall of the quartz tube were observed. The CNTs mat from the quartz tube was collected by scraping the tube walls. The as-obtained CNTs powder and carbon fibers (hair-like structures) were investigated by FTIR and Raman spectroscopy techniques, optical and scanning electron (SEM) microscopy and TGA techniques. Results of these investigations are presented and discussed in this chapter.

5.1 Effect of Growth Temperature

TGA plots for the first set of samples are shown in Fig. 5.1. From the graphs in Fig. 5.1(b) it can be seen that the amount of residual mass decreases with increasing growth temperature. The residual mass is a compound of iron and oxygen i.e. iron oxide. Less residual mass means that the residues of iron catalyst on CNTs decreased with increasing growth temperature. This feature was also supported by the fact that the oxidation temperature increased with increasing growth temperature, which is an indication of more graphitization. However, the less product yield at

higher temperatures could be due to the secondary flow of the material, caused by the temperature gradient which pushes more carbon onto a catalyst particle while higher temperatures favor its graphitization/adhesion resulting in a thick and long carbon fiber. TEM images of sample grown at higher temperatures (see Fig. 5.2) show bead like structures forming a fiber. The EDX of this fiber revealed that huge amount of carbon surround a small iron particle. In order to discourage this accumulation of carbon the carrier gas flow rate was varied in set-II and its effect was investigated.
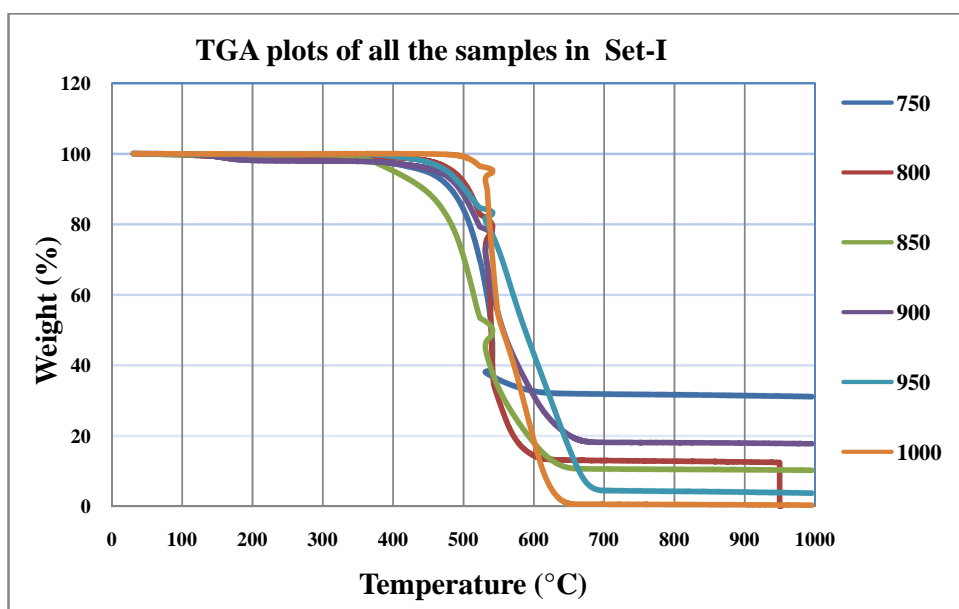
(a)
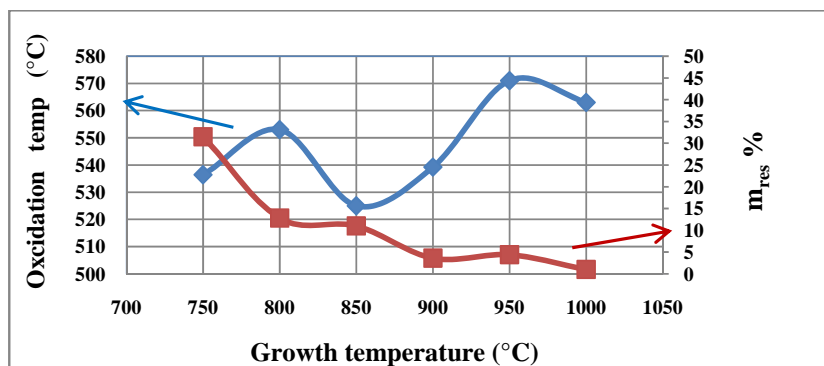
(b)

Figure 5.1 (a) TGA plots of all the samples in Set-I, (b) graphs of variation of oxidation temperature and residual mass with the growth temperature.
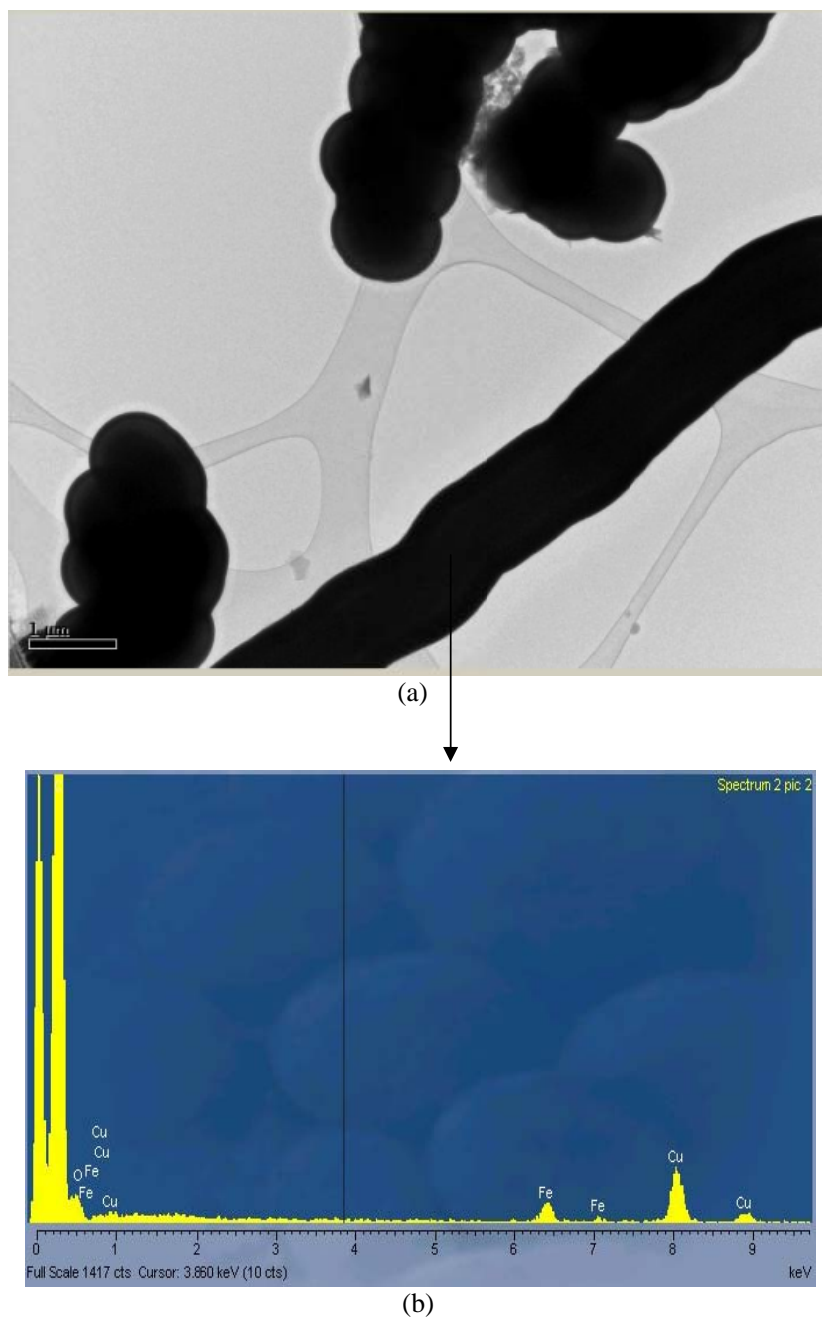
(a)

(b)

Figure 5.2 (a) TEM image of Sample # 6 (Growth temperature = 1000°C) and (b) EDX
analysis of material shown in part (a).

Raman spectra of this set of samples are shown in Fig. 5.3(a). A sharp peak around $1190cm^{-1}$ and the two small peaks around $135cm^{-1}$ and $275cm^{-1}$ are instrumental artifacts due to filter problems. Two characteristic peaks of CNTs,

namely D and G were observed at 1580 cm^{-1} ($\pm$5cm^{-1}) and 1325 cm^{-1} ($\pm$5cm^{-1}) respectively. The height of D and G peaks decreased with increasing growth temperature which is again in support of the above mentioned accumulation of amorphous carbon at higher temperatures.
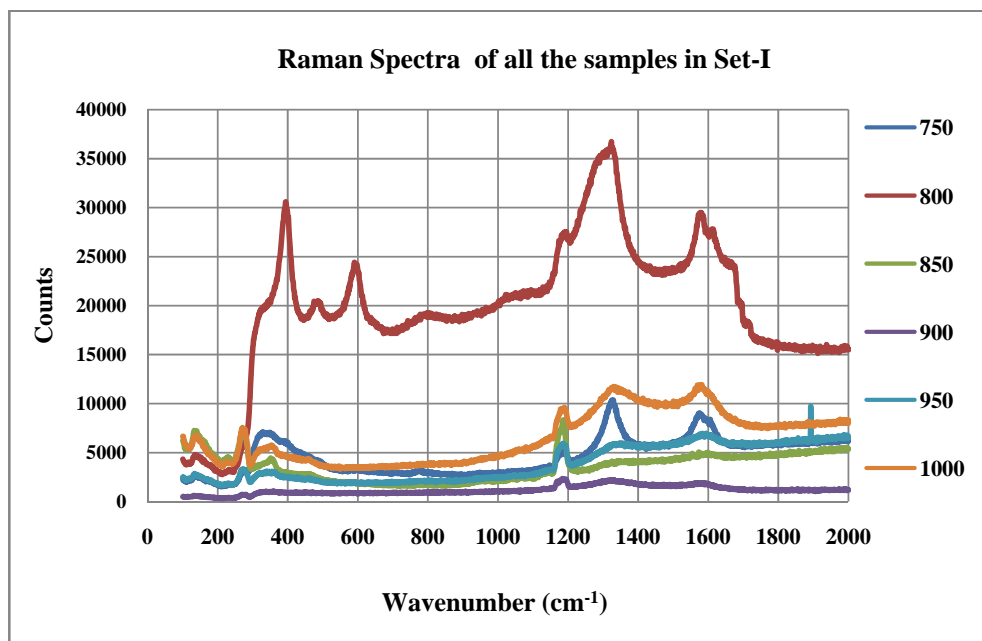
(a)
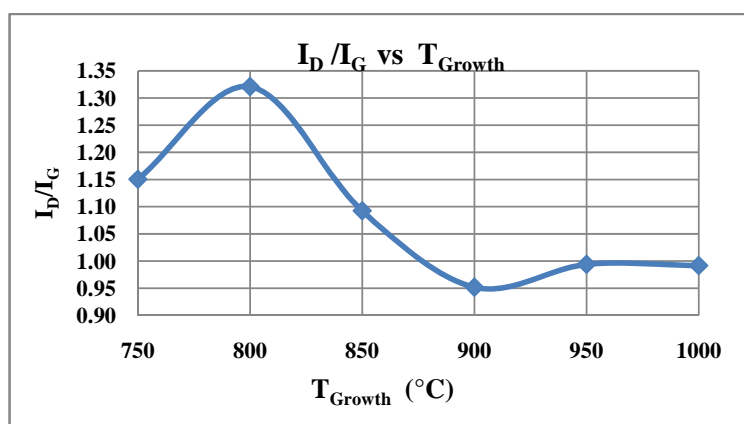
(b)

Figure 5.3 (a) Raman spectra of all samples in Set-I, (b) and graph of I_G/I_D ratio.

FTIR spectra for the first set of samples are shown in Fig. 5.4. No absorption

peak was observed and there was strong absorption at low wavenumber which can be attributed to the bundle effect because as-grown CNTs tend to form bundles due to van der Walls forces between them. The theoretically predicted peaks for individual CNT are calculated based on an isolated CNT. Transmission IR spectra of CNTs samples on Si substrate were subsequently taken with a single sample holder (the effect of the Si substrate was included in the background).
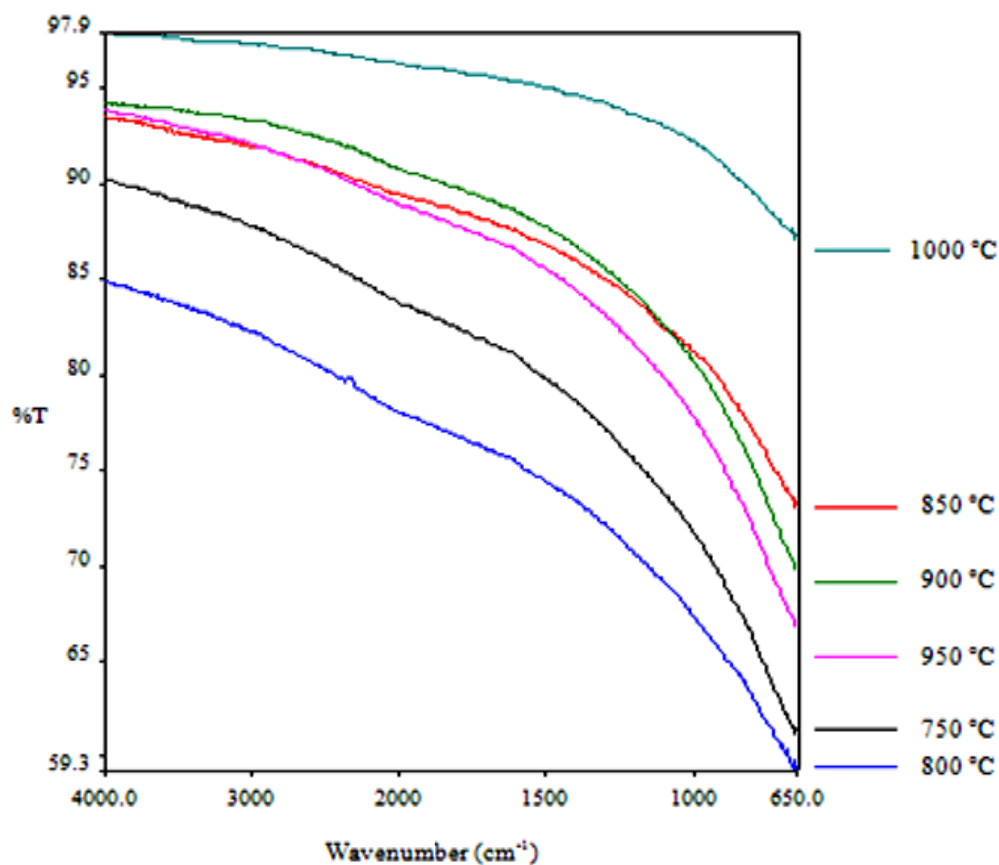

Figure 5.4 FTIR spectra of all samples in set-I (growth temperature variation)

This time the transmission was nearly zero with the signal increasing at lower wavenumbers, which was opposite to what was observed with the HATR accessory. Finally, small quantities of powder from each sample were dispersed ultrasonically in methanol in small glass vials. A drop from each mixture was poured onto separate Si

substrate and left to dry overnight (nearly 14 hours). Methanol evaporated and the CNTs powder was stuck onto the Si substrate in the form of a broken and non-uniform film. FTIR spectra of these samples were taken using a single sample holder (again, the Si substrate contribution was included in the background). This time some absorption peaks were observed indicating some compounds of carbon, hydrogen and oxygen but no CNT characteristic peak was observed. More work on IR study of CNTs is required.

5.2 Effect of Carrier Gas Flow Rate

In order to discourage the accumulation of carbon, the carrier gas flow rate was changed from 10sccm to 100sccm in set-II and its effect on the quality of the samples was investigated. It was found that higher flow rates reduced the accumulation of amorphous carbon but decreased the product yield.
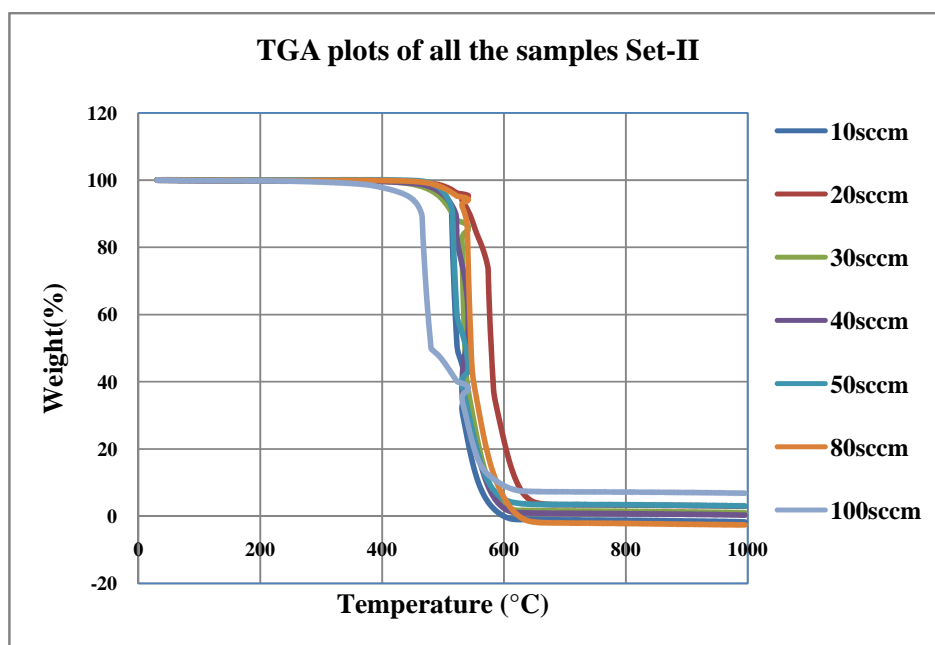

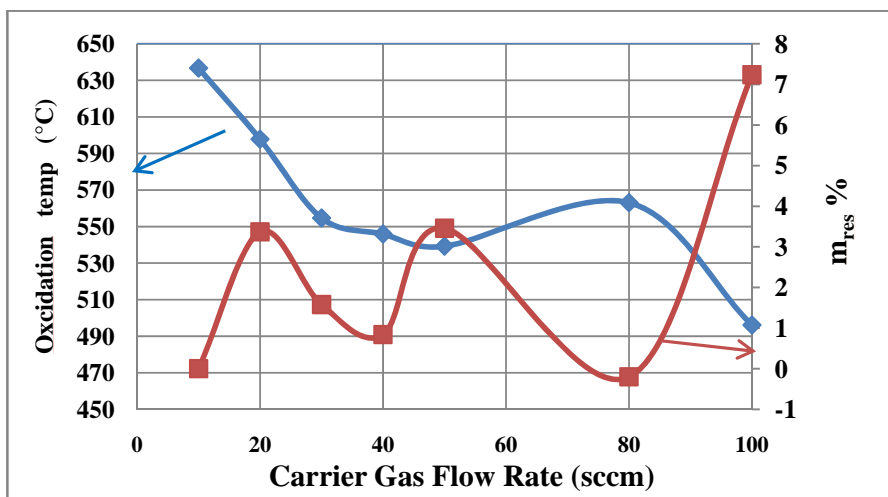Figure 5.5 (a) TGA of all the samples in Set-II

Figure 5.5 (b) Plots of variation of oxidation temperature and residual mass.

Higher gas flow pumped out the material from the pyrolysis zone, with less residence time. TGA results indicated that the oxidation temperature was almost unaffected by the change in carrier gas flow rate. The residual mass showed an oscillatory behavior when changing carrier gas flow rate, and had minimum value at 40 and 80sccm (see Fig.5.5 (b)). The product yield was high at 40sccm and low at 80sccm.
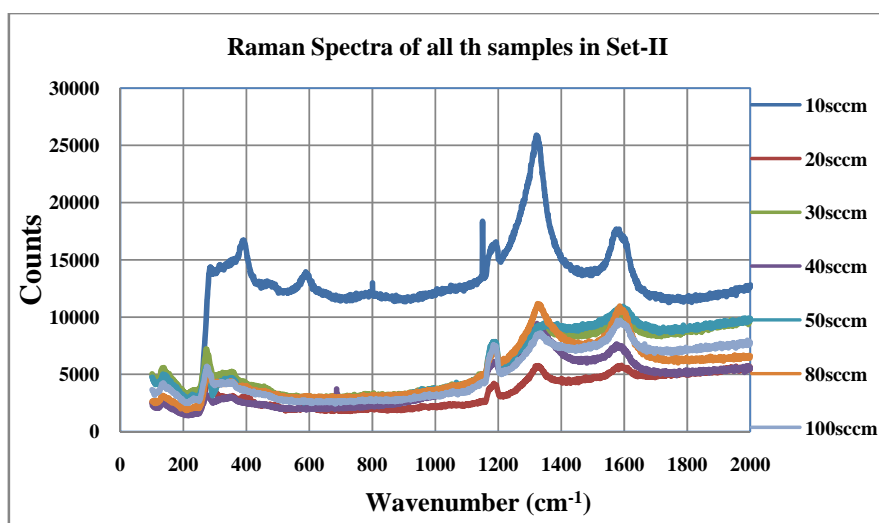

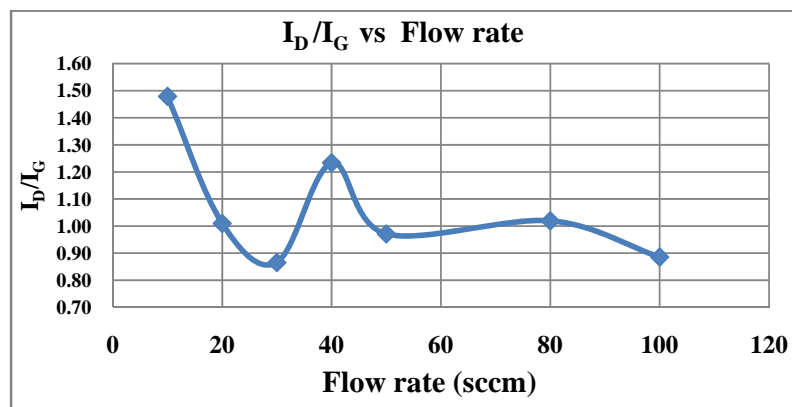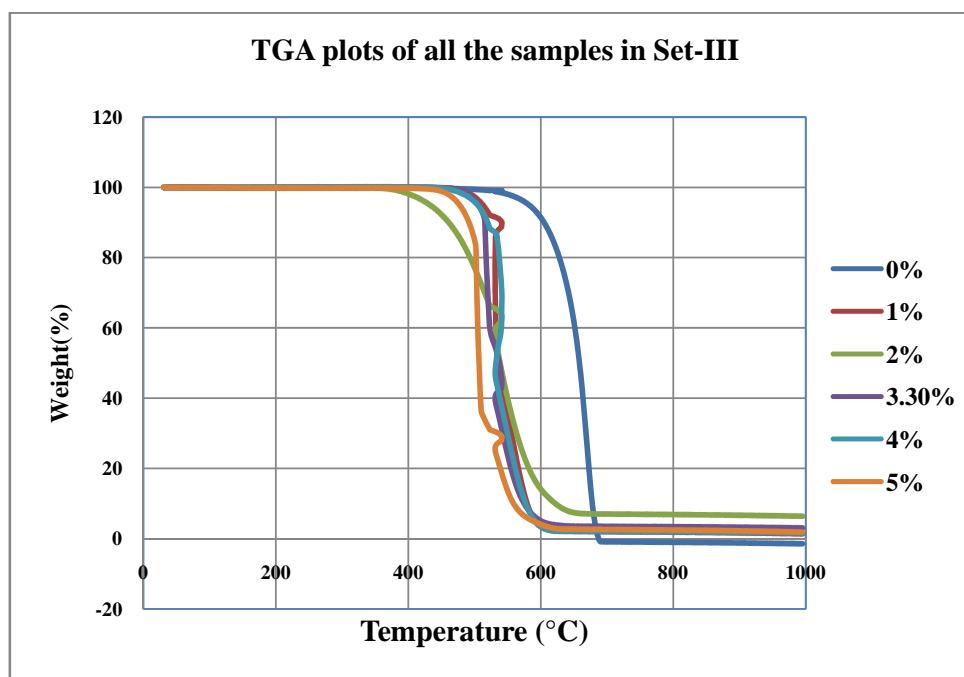Figure 5.6 (a) Raman spectra of all samples in set-II

Figure 5.6 (b) Graph of I_D/I_G versus carrier gas flow rate.

Raman studies of this set of samples revealed that the quality of the product improved with increasing flow rate with one exception from this trend for the sample grown at 40sccm. FTIR spectra for this set of samples were similar to the ones in first set where no peak was observed.

5.3 Effect of catalyst concentration

A variation in the residual mass was observed from TGA graphs of set-II. In order to investigate this variation in the residual mass, the effect of the catalyst concentration was studied in set-III. From TGA graphs of all samples in set-III (shown in Fig. 5.7), it was found that the sample with 0% catalyst concentration had a very high oxidation temperature as compared to the other samples in this set. This suggests that the sample with 0% catalyst concentration was graphitic or black carbon. The residual mass signal showed an oscillatory behavior when changing catalyst concentration with minimum at 1% and 4%.

(a)
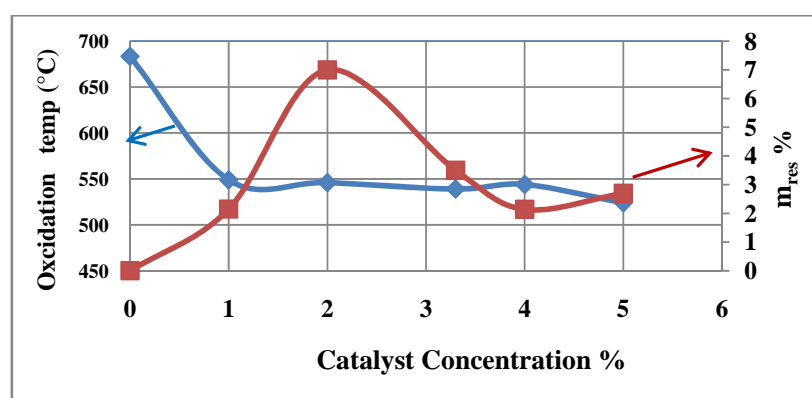
(b)

Fig. 5.7 (a) TGA graphs of all samples in set-III , (b) plots of variation of oxidation temperature and residual mass.

Raman spectra of this set of samples are shown in Fig. 5.8. For the sample with 0% catalyst concentration a very broad and high D peak and a high G peak was observed. The graph of I_D/I_G (i.e., the ratio of intensities of D and G peaks in the Raman spectrum) showed minimum values for samples with 1% and 4% catalyst concentration, consistent with TGA results, indicating that these samples were good quality as compared to other samples in the set.
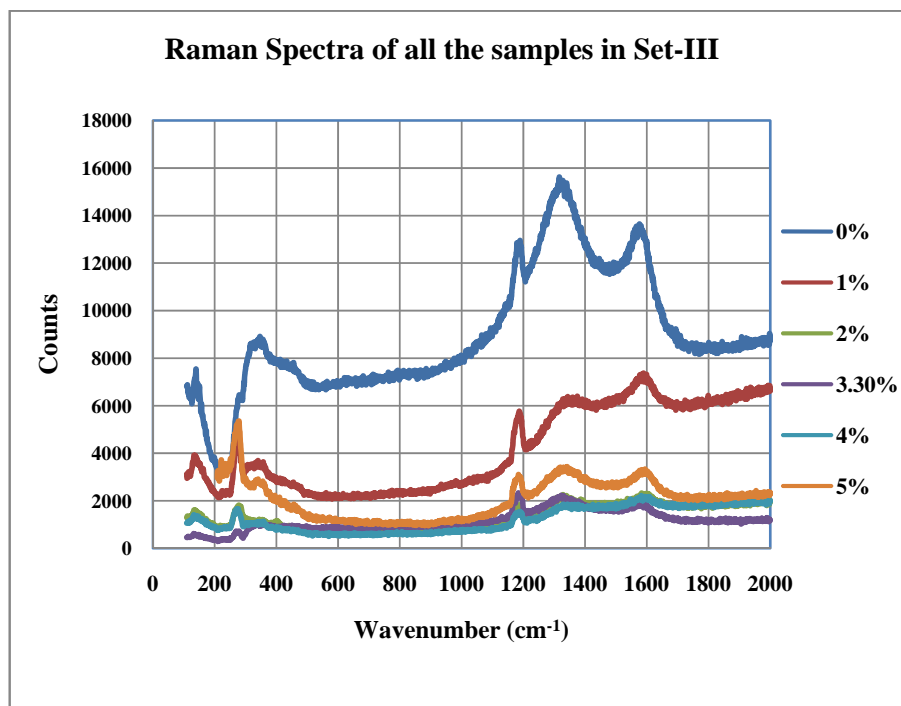
(a)
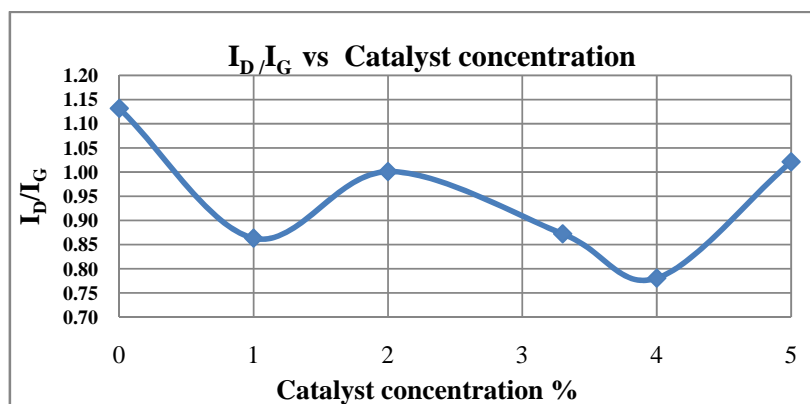
(b)

Figure 5.8 (a) Raman spectra of all samples in set-III (b) graph of I_G/I_D ratio of D and G peaks of spectra in (a).

FTIR spectra of samples in set-III were similar to the ones for the first two sets, with no peak.

5.4 Electron Microscopy Results

SEM images of samples # 2 and # 3 are shown in Figs. 5.9 and 5.10 at different magnifications. From Fig.5.9 it can be seen that the height of the dense and aligned CNT mat is nearly 500µm.
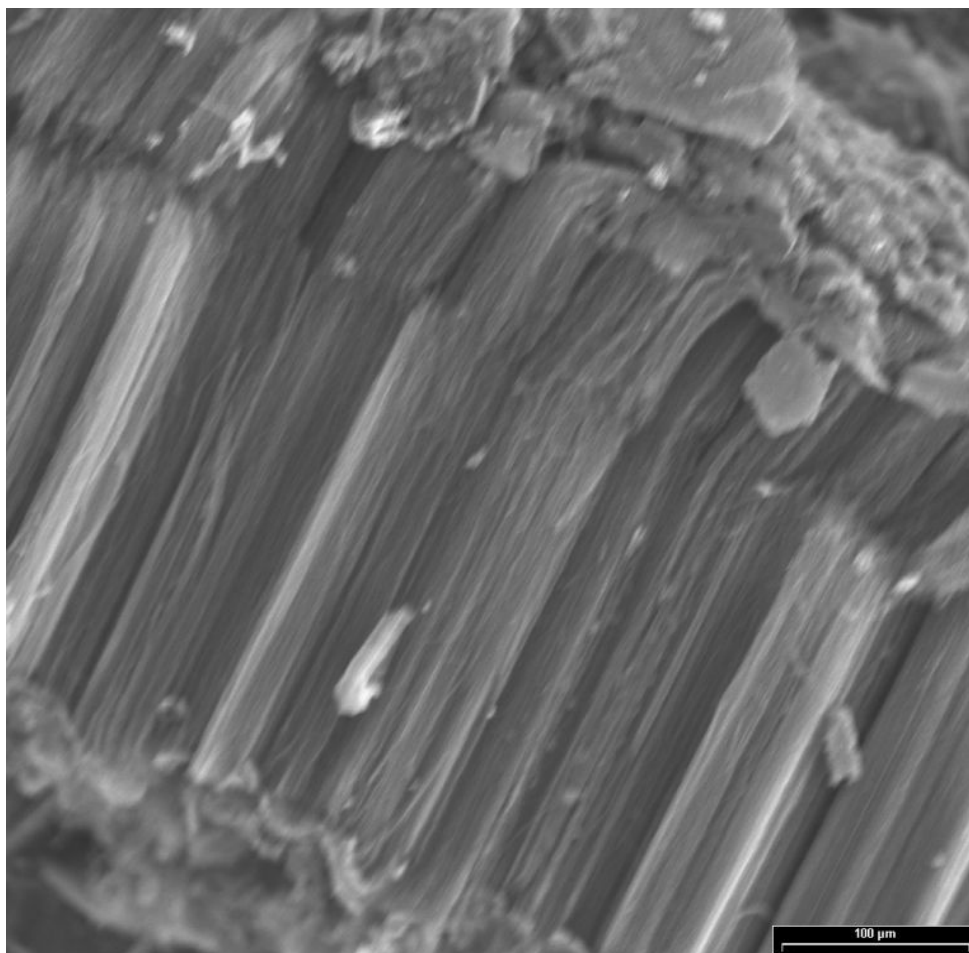
Figure 5.9 SEM micrograph CNTs mat (sample # 2).
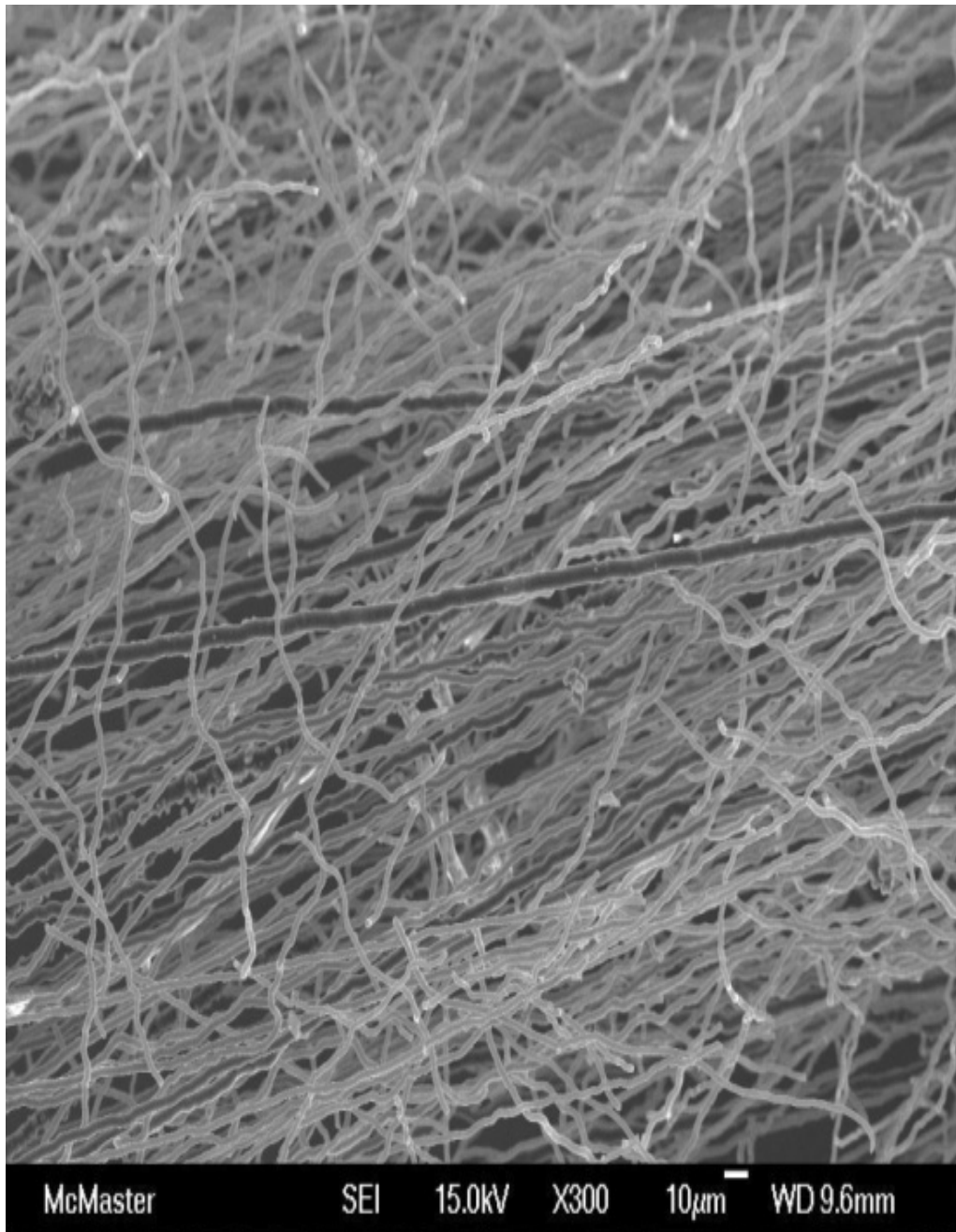
Figure 5.10 SEM micrograph of CNTs/CNFs in sample #3.
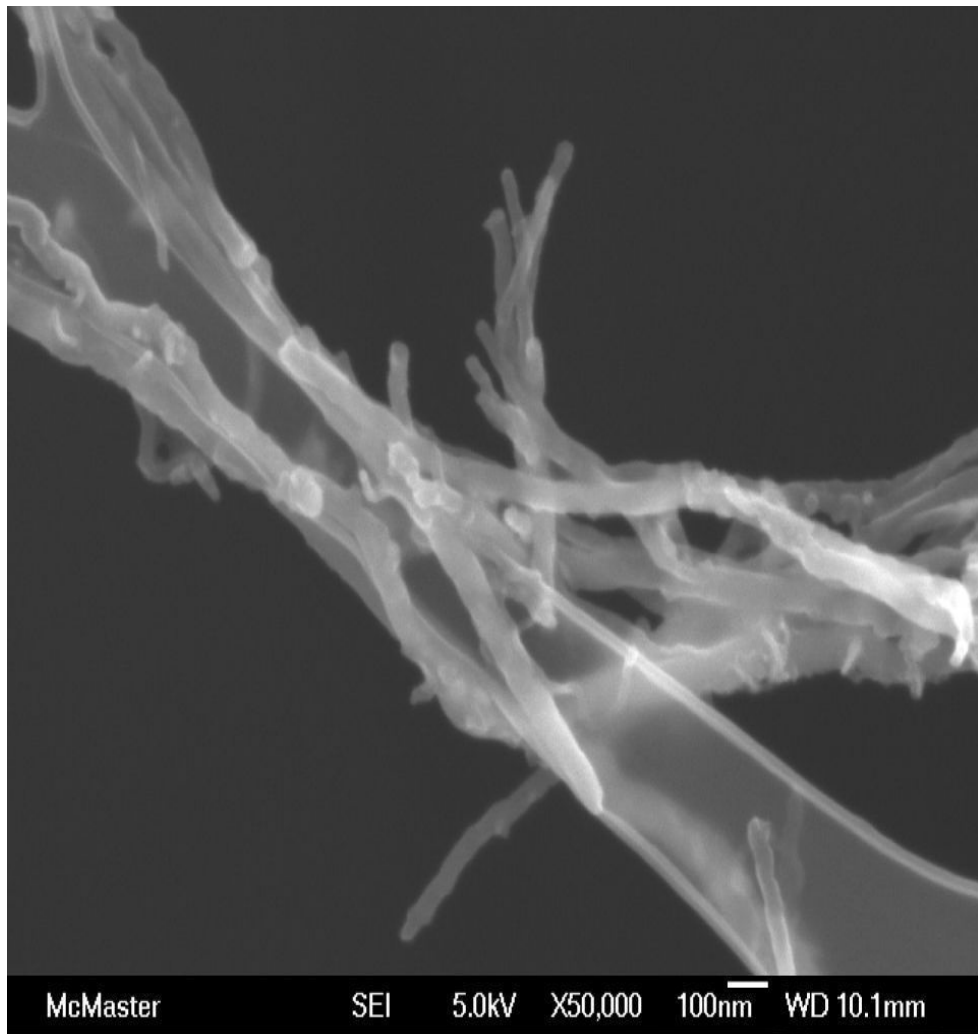
Figure 5.11 SEM micrograph (of sample # 2) CNTs at 100000 times magnification.
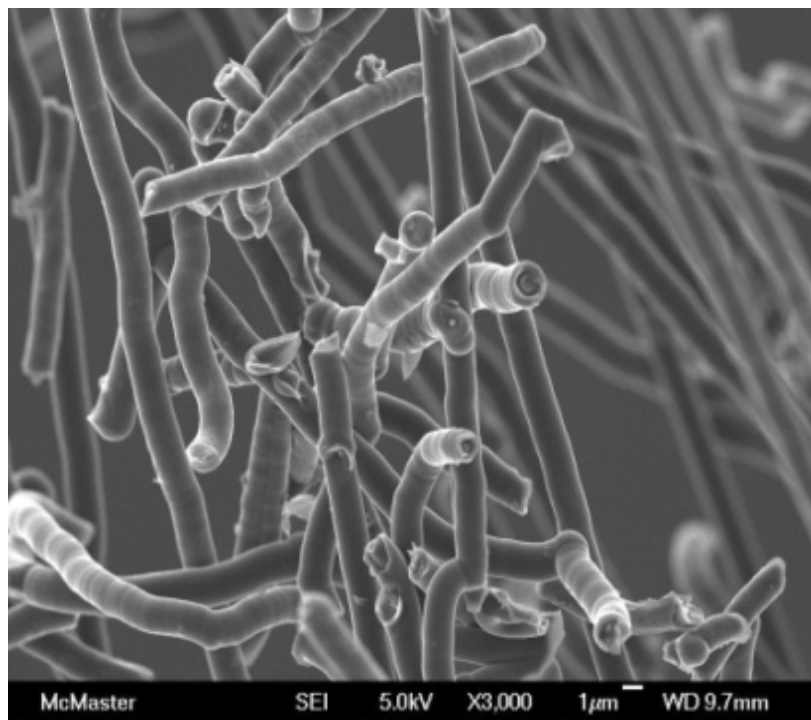
(a)
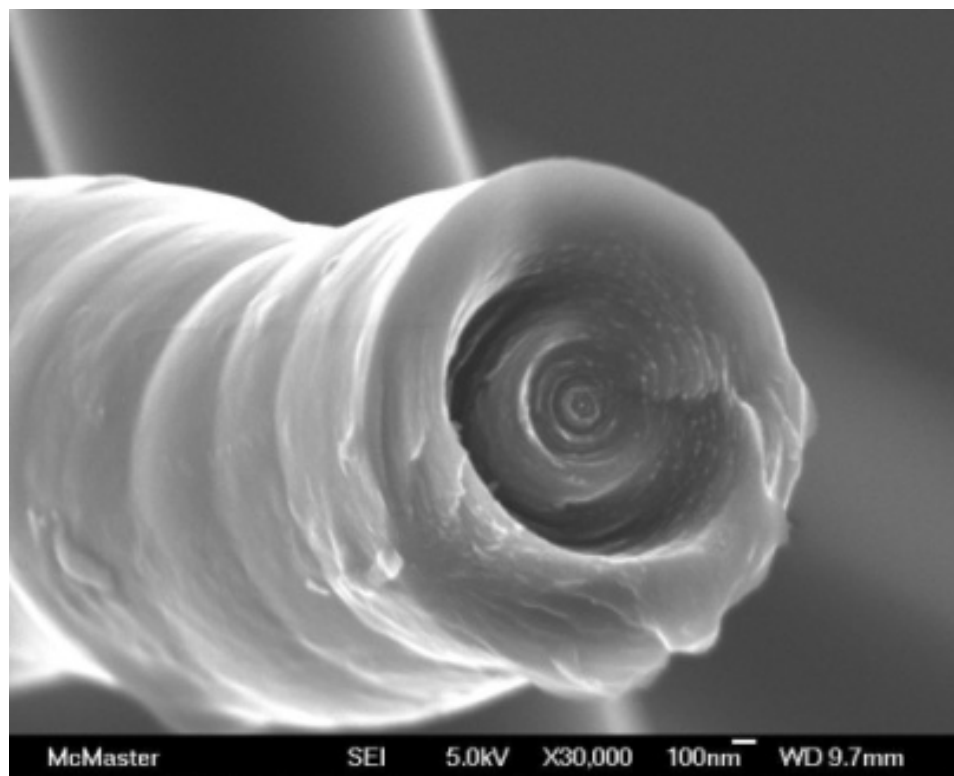
(b)
Figure 5.12 (a) SEM micrograph of branched CNFs/MWCNTs,
(b) magnified view of end of a MWCNT.
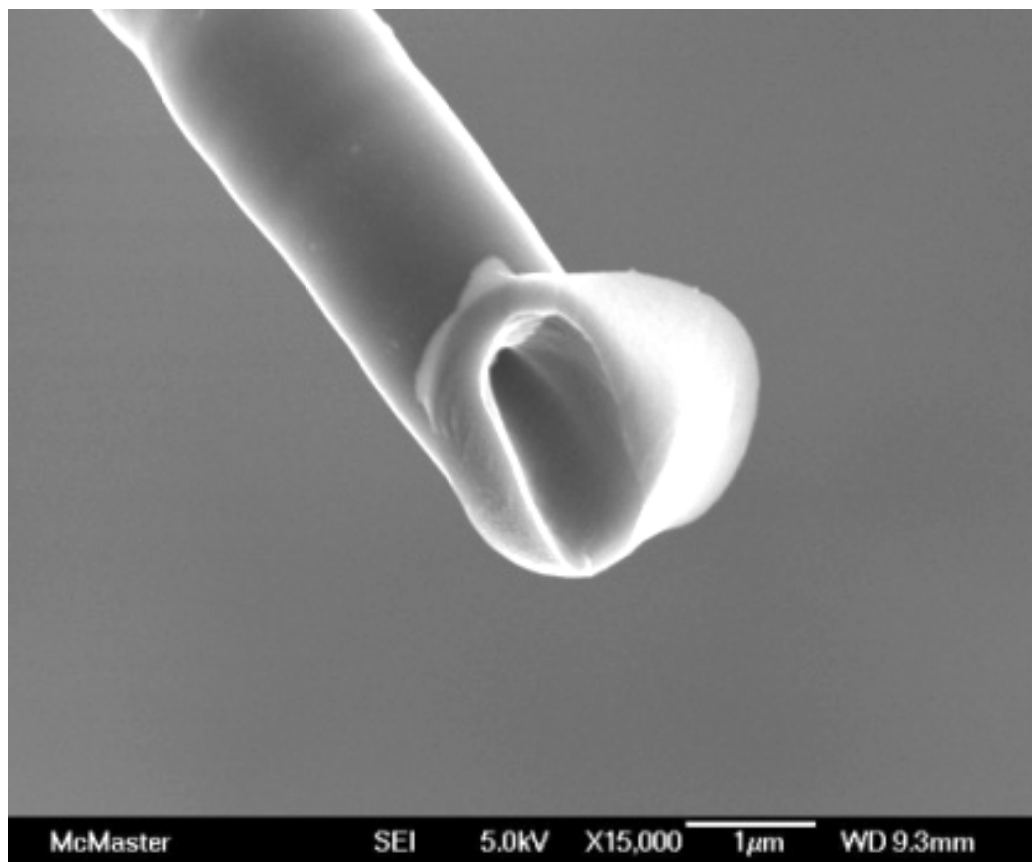
Figure 5.13 SEM micrograph of crossection of a MWCNTs

In Fig. 5.12 (b) and 5.13 two magnified cross-sectional views of cylindrical and tubular structures are shown. In order to further clarify the nature of these structures, i.e. MWCNT or CNF, TEM micrographs were taken. (see Figs. 5.14-5.18). These TEM images clearly show that these structures are in fact MWCNTs. EDX analysis of the dark spots on the tubes revealed that these were actually trapped iron catalyst particles (or likely Fe_3C), as shown in Fig. 5.15. TEM images of another sample (#8) along with EDX are shown in Fig. 5.16., again showing the MWCNTs along EDX of the catalyst particle.
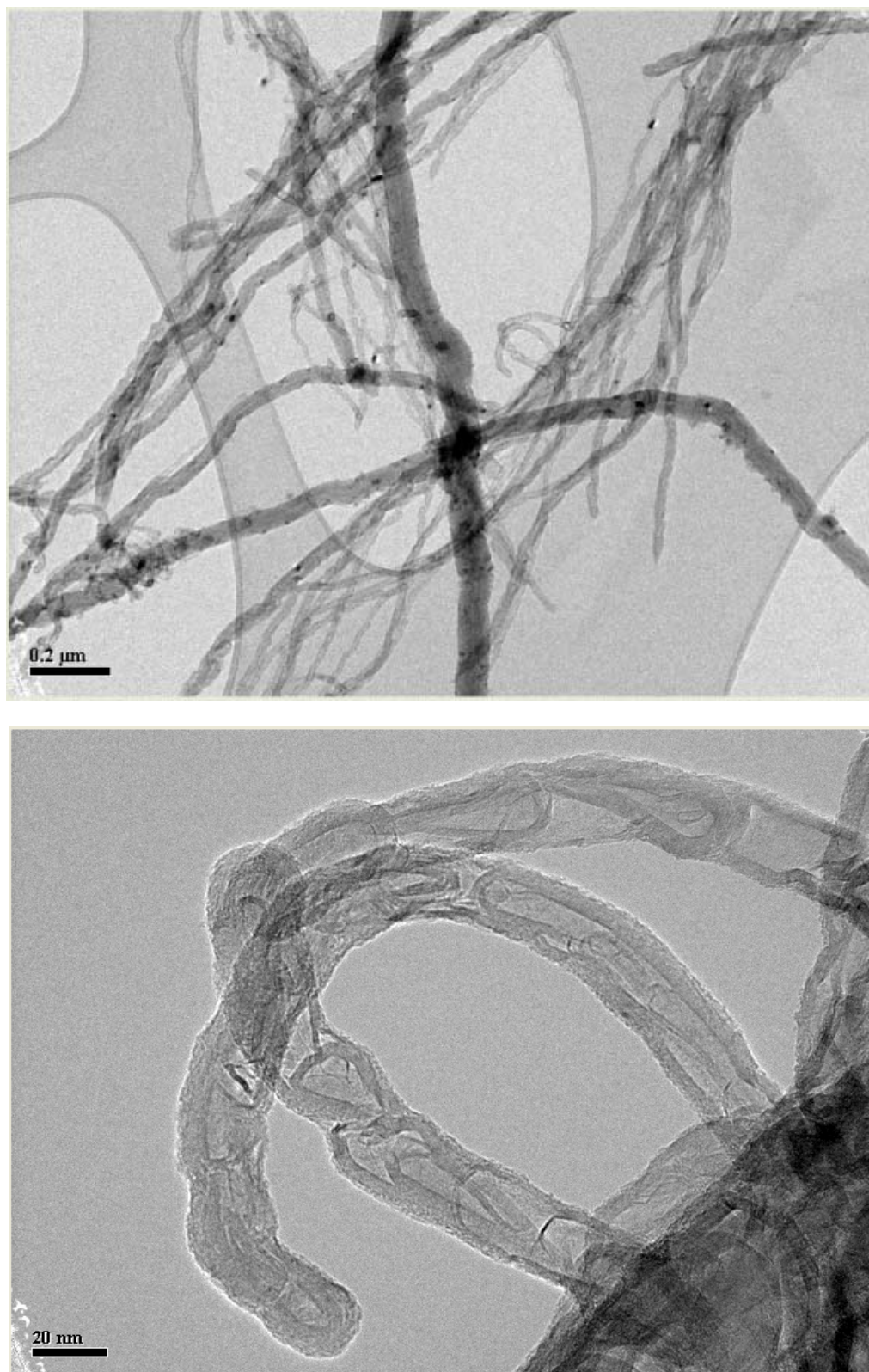
Figure 5.14 TEM micrographs at different magnifications, showing MWCNTs.
(sample # 2 CNT05-02-09 800)
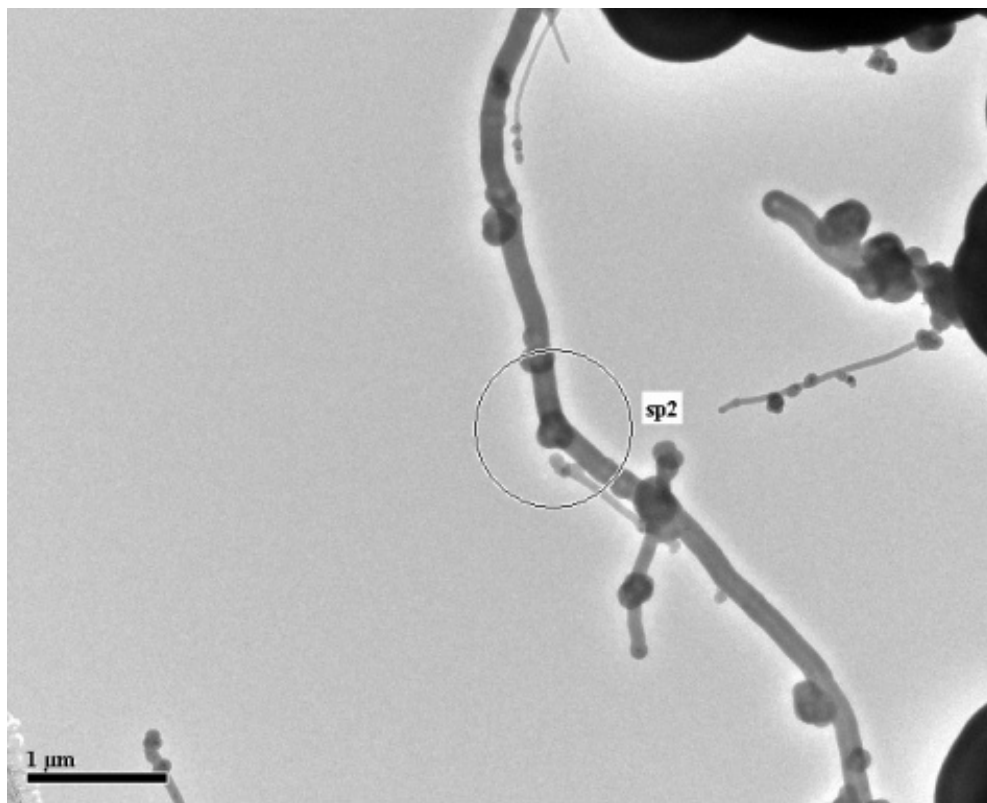
(a)
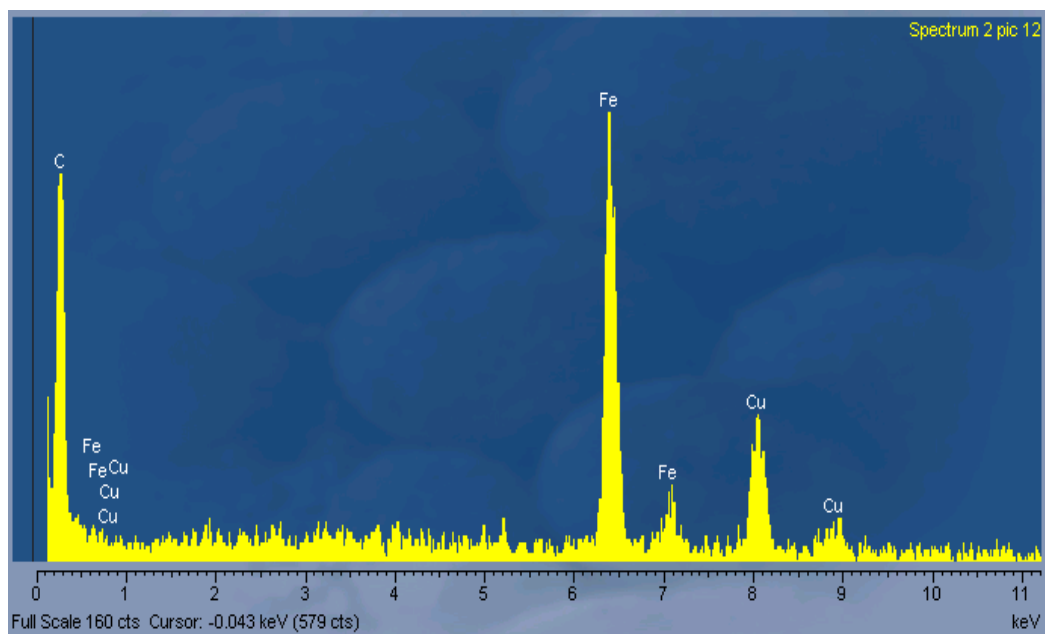
(b)

Figure 5.15 (a) Closer view of a MWCNT with dark spots (b) EDX of CNT shown in (a), suggests that the dark spot on the tube consists of Fe catalyst particle.

(a)

(b)   (c)
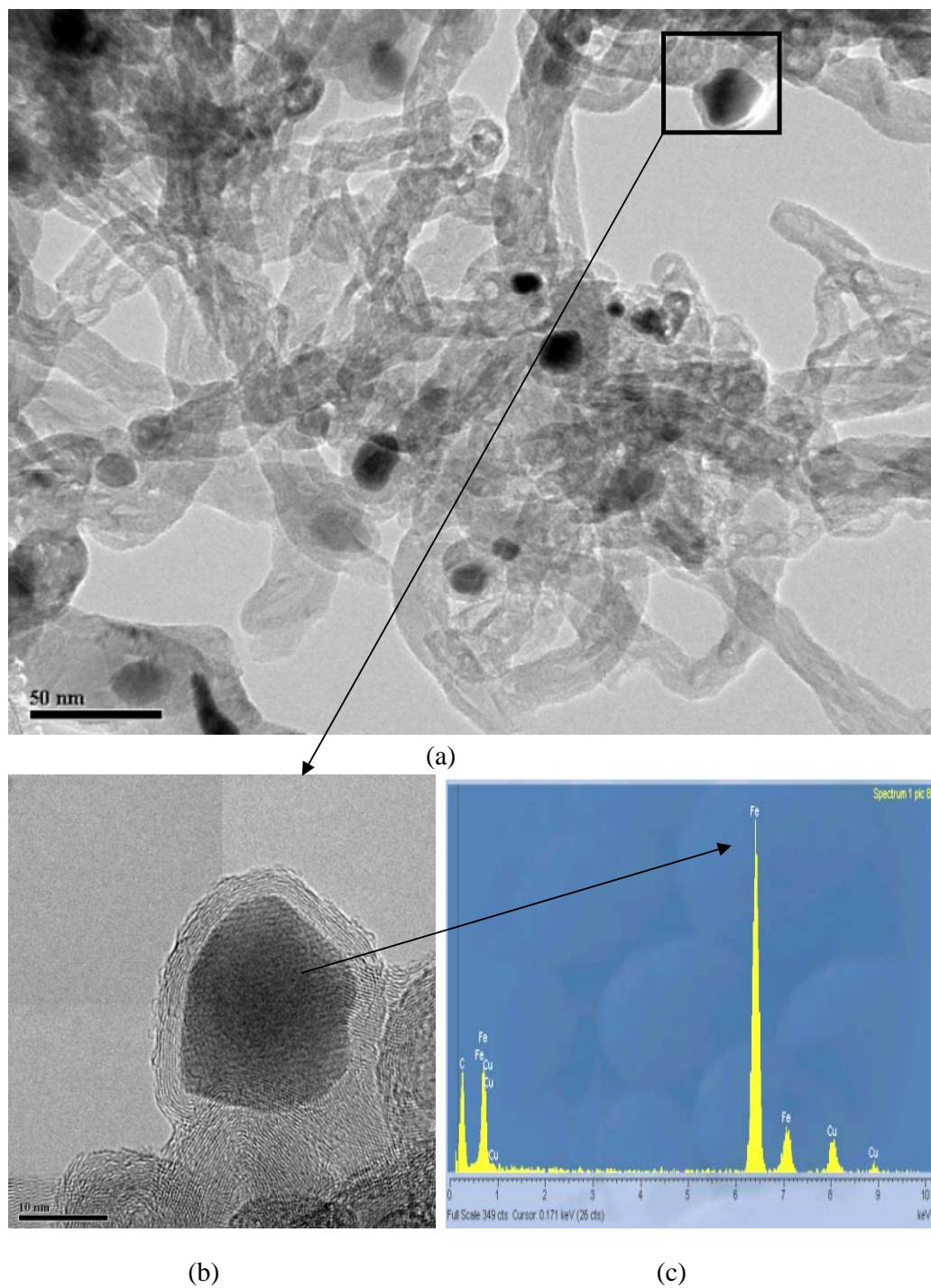
Figure 5.16 TEM micrographs of Sample # 8 (grown at 900°C) at different
         magnifications (a and b) and (c) EDX of material at the end of MWCNT
         shown in (b).

HRTEM images of sample # 18, shown in Fig. 5.16, suggest that most of the CNTs are multiwall, however there are some single wall (see Fig.5.17a) and double wall (see Fig, 5.18) CNTs in the bundle.

Single-wall carbon nanotube

(a)

Multi-wall carbon nanotube

10 nm
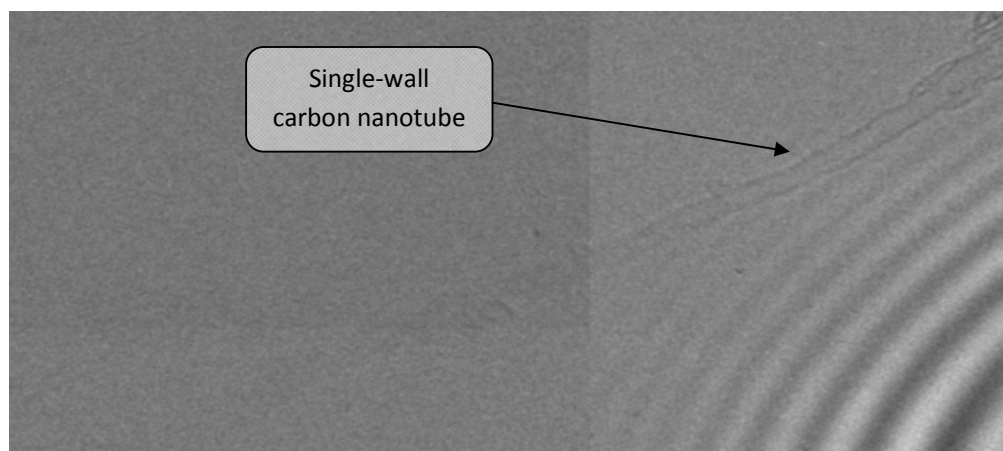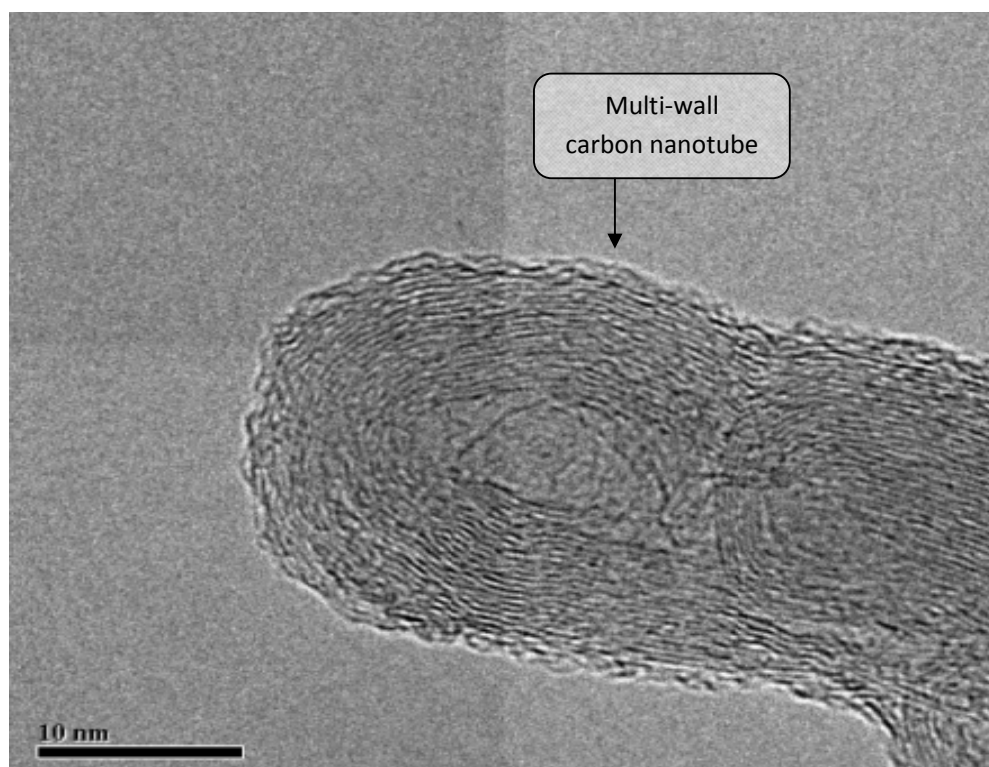
(b)

Figure 5.17 HRTEM of (a) SWCNT (CNT19-05-09 40sccm sample), (b) MWCNTs.
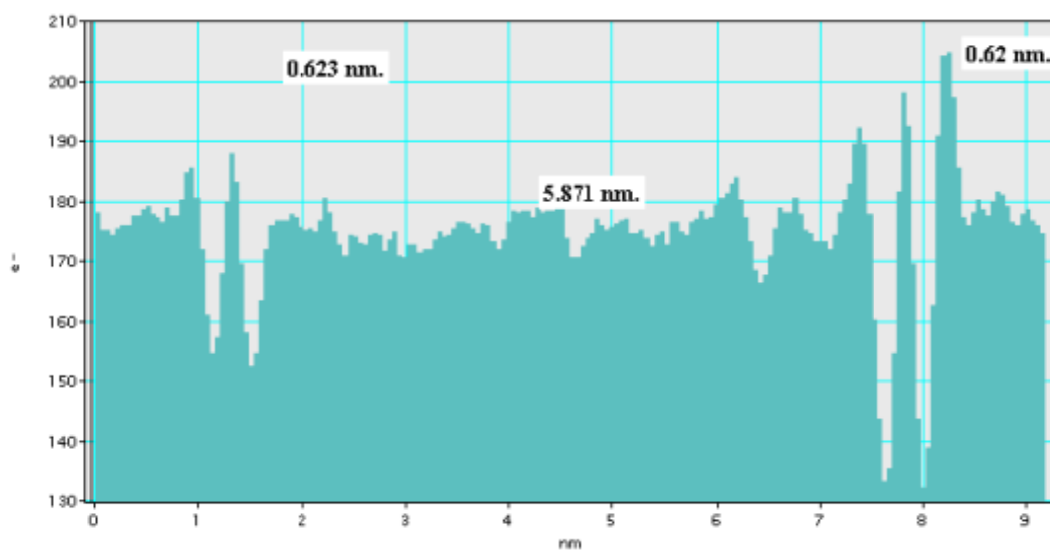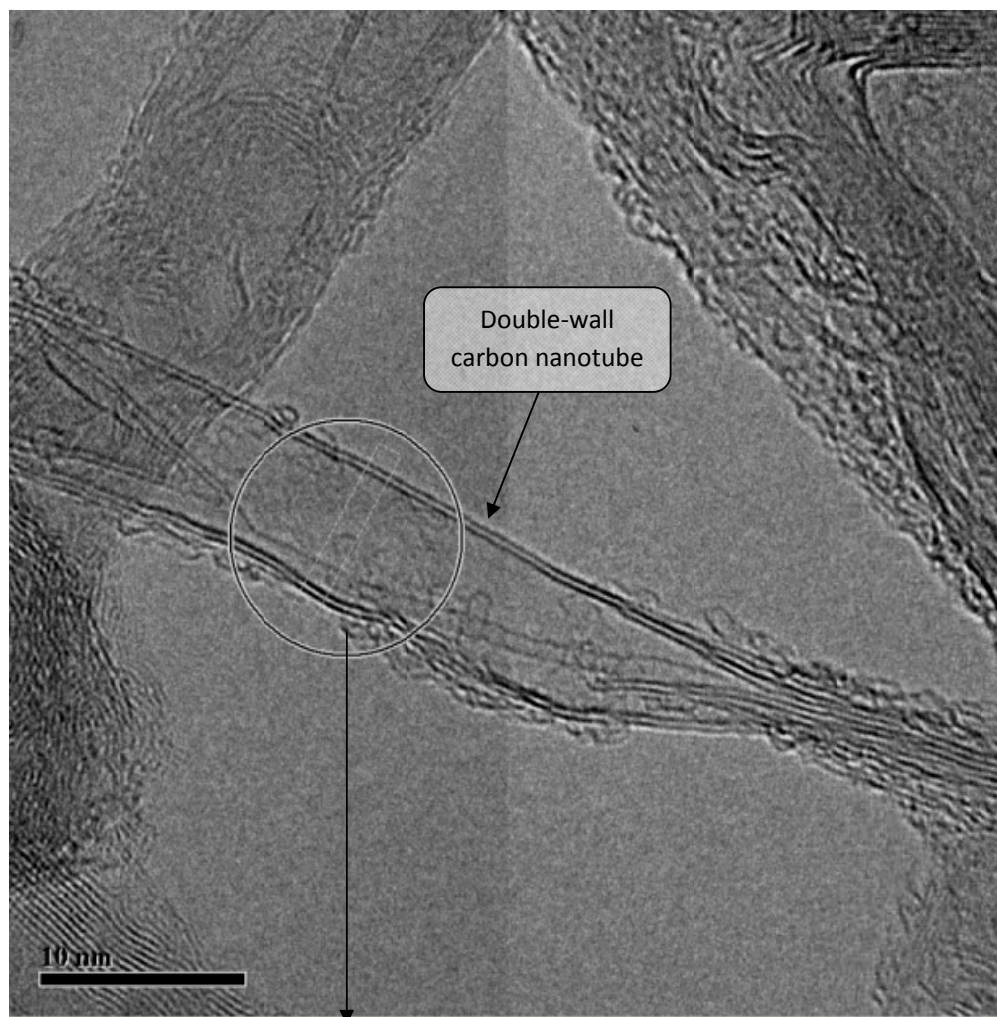
Figure 5.18 HRTEM of DWCNT with calculated inter-wall separation of 0.62nm and internal diameter of inner tube 5.871nm

5.5 CONCLUSION

Carbon nanotubes (CNTs) can be grown from mixtures of camphor and ferrocene, using chemical vapor deposition (CVD) technique. Growth process of CNTs was affected by a number of growth parameters. For temperatures more than 900°C the quality of CNTs decreased and a mixture of small carbon fibers, carbon spheres and metal particles were observed. High flow rate of carrier gas resulted in low yield. A mixture of single wall, double wall and multiwall CNTs were grown. CNTs grew on both c-Si and Quartz substrates but the density of CNTs was less on the substrates surfaces as compared to their density on the edges of the substrates. Comparing the results of present work with those reported in literature, it was found that the present CVD setup is simple and economical and good quality samples were grown at 800°C pyrolysis temperature, 80sccm carrier gas flow rate and 4% catalyst concentration.

5.6 Future Work

FTIR spectra of all samples didn't show any prominent peak. In fact, the high concentration of the material resulted in a very week signal. Future work is needed to improve the quality of the signal. KBr pellets with a small quantity of CNT powder should be used for better transmission IR signal.

The preferential and directional growth of hair-like structure of CNTs/CNFs on substrate edges also needs to be explored. A further step towards achieving a better understanding of the growth process is to improve the present CVD setup as suggested in chapter 4.

References:

[1] Science of fullerenes and carbon nanotubes by M. S. Dresselhaus, G. Dresselhaus, P. C. Eklund. Academic Press, California, USA, 1996.

[2] Carbon Nanotubes: Science and Applications, edited by M. Meyyappan, CRC press, Florida, USA, 2005.

[3] S.Iijima, Nature 354 (1991) 56.

[4] Introduction to Nanoscience by Gabor Louis Hornyak, Joydeep Dutta, Harry F. Tibbals and Anil K. Rao. CRC press, Florida, USA, 2008.

[5] T. Belin and F. Epron, Materials Science and Engineering B 119 (2005) 105.

[6] P. Avouris, Chemical Physics 281 (2002) 429.

[7] Carbon nanotubes: Properties and applications edited by M.J. O'Connell, CRC Press, Florida, USA, 2006.

[8] M.S. Dresselhaus, G. Dresselhaus and A. Jorio, Annual Review, Matter. Res. 34 (2004) 247.

[9] Morinobu Endo, Michael S. Strano, and P. M. Ajayan, Carbon Nanotubes, Chapter 16, pp. 13 – 62.

[10] Axel Hagen and Tobias Hertel, Nano Letters, 3 (2003) 383.

[11] Yung Joon Jung, Nanomanufacturing Handbook, Chapter 4, pp 81 – 106.

[12] D.S. Bethune, R. D. Johnson, J. R. Salem, M. S. de Vries and C. S. Yannoni, Nature, 363 (1993) 605.

[13] S. Iijima, and T. Ichihashi, Nature, 363 (1993) 603.

[14] T.W.Ebbesn and P.M.Ajayan, Nature 358 (1992) 220.

[15] Zujin Shi, Yongfu Lian, Xihuang Zhou, Zhennan Gua, Yaogang Zhang, Sumio Iijima , Lixia Zhou , Kwok To Yue , Shulin Zhang, Carbon, 37 (1999) 1449.

[16] Yoshinori Ando and Xinluo Zhao, New Diamond and Frontier Carbon Technology, 16 (2006) 3.

[17] Shigeo Maruyama, Ryosuke Kojima, Yuhei Miyauchi, Shohei Chiashi, Masamichi Kohno, Chem. Phys. Lett., 360 (2002) 229.

[18] M Meyyappan, Lance Delzeit, Alan Cassell1 and David Hash, Plasma Sources Sci. Technology. 12 (2003) 205.

[19] G. Ortega-Cervantez, G. Rueda-Morales, J. Ortiz-Lo´pez, Microelectronics Journal, 36 (2005) 495.

[20] Biao Wang, Xinyu Liu, Hongmin Liu, Dexin Wu, Huaping Wang, Jianming Jiang, Xianbao Wang,a Ping-an Hu,a Yunqi Liu and Daoben Zhu, J. Mater. Chem., 13 (2003) 1124.

[21] Cınar Oncel and Yuda Yurum, Fullerenes, Nanotubes, and Carbon Nanostructures, 14 (2006) 17.

[22] Mukul Kumar, Keita Kakamu, Tsugio Okazaki, Yoshinori Ando, Chemical Physics Letters, 385 (2004) 161.

[23] Rong Xiang, Guohua Luo, Zhou Yang, Qiang Zhang, Weizhong Qian, Fei Wei, Materials Letters 63 (2009) 84.

[24] Xianming Liu, Keith H.R. Baronian, Alison J. Downard, Carbon 47 (2009) 500.

[25] Carole E. Baddour, Faysal Fadlallah, Deniz Nasuhoglu, Reema Mitra, Leron Vandsburger, Jean-Luc Meunier, Carbon 47 (2008) 313.

[26] Simone Mussoa, Samuele Porroa, Mauro Giorcellia, Alberto Tagliaferro, Physica E 37 (2007) 16.

[27] J. Justin Gooding, Electrochimica Acta, 50 (2005) 3049.

[28] Charanjeet Singh, Milo S.P. Shaffer, Alan H. Windle, Carbon 41 (2003) 359.

[29] Simone Musso, Samuele Porroa, Massimo Rovereb, Mauro Giorcellia, Alberto Tagliaferro, Journal of Crystal Growth 310 (2008) 477.

[30] Roman Brukh, Somenath Mitra, Chemical Physics Letters 424 (2006) 126.

[31] H. Kataura, Y. Kumazawa, Y. Maniwa, I. Umezu, S. Suzuki, Y. Ohtsuka and Y. Achiba, Synthetic Metals, 103, (1999), 2555.

[32] http://teaching.shu.ac.uk/hwb/chemistry/tutorials/molspec/irspec1.htm

[33] A. M. Rao, E. Richter, Shunji Bandow, Bruce Chase, P. C. Eklund, K. A. Williams, S. Fang, K. R. Subbaswamy, M. Menon, A. Thess, R. E. Smalley, G. Dresselhaus, M. S. Dresselhaus, Science 275 (1997) 187.

[34] http://www.msel.nist.gov/Nanotube2/Practice%20Guide_Section%202_TGA.pdf

[35] Sivaram Arepalli, Pavel Nikolaev, Olga Gorelik, Victor G. Hadjiev, Williams Holmes, Bradley Files, Leonard Yowell, Carbon 42 (2004) 1783.

[36] Marko Burghard, Surface Science Reports 58 (2005) 1.

[37] P. C. Eklund, J.M. Holden and R.A.Jishi, Carbon 33, 7 (1995) 959.

[38] D.E. Newbury and D.B. Williams, Acta mater. 48 (2000) 323.

[39] S. D. M. Brown, A. Jorio, and P. Corio, Physical Review B 63 (2001) 155414.

[40] S. Costa, E. Borowiak-Palen, M. Kruszyñska, A. Bachmatiuk, R J. Kaleńczuk, Materials Science-Poland 26 2 (2008) 433.

Appendix
Copy Rights Permissions

Dear Muhammad Shafiq Ahmed,

We give you the permission to use this figure in your M.Sc. thesis. Please indicate the correct citation.

Best regards,

Claus Ascheron

Dr. habil. Claus E. Ascheron
Springer Science+Business Media
Physics Editorial IV
Executive Editor Physics
Tiergartenstr. 17 | 69121 Heidelberg | Germany
tel.:   +49-6221-487-8675
fax: +49-6221-487-8995
claus.ascheron@springer.com
http://www.springer.com

Von: Muhammad Shafiq Ahmed [mailto:MuhammadShafiq.Ahmed@uoit.ca]
Gesendet: Dienstag, 4. August 2009 17:17
An: Ascheron, Claus, Springer DE
Betreff: Copyright permission request

Date: August 4, 2009

Publisher: Springer-Verlag Berlin Heidelberg

Dear Editor,
I am preparing my M.Sc. thesis for submission to the Office of Graduate Studies at the University of Ontario Institute of Technology (UOIT) in Oshawa, Ontario, Canada. I am seeking your permission to include a manuscript version of the following figure in the thesis:

Carbon Nanotubes : Topics Appl. Physics 111, 13–62 (2008)

© Springer-Verlag Berlin Heidelberg 2008

Figure No. 2 on page 22

Canadian graduate theses are reproduced by the Library and Archives of Canada (formerly National Library of Canada) through a non-exclusive, world-wide license to reproduce, loan, distribute, or sell theses. I am also seeking your permission for the material described above to be reproduced and distributed by the LAC(NLC). Further details about the LAC(NLC) thesis program are available on the LAC(NLC) website (www.nlc-bnc.ca).
Full publication details and a copy of this permission letter will be included in the thesis.
Yours sincerely,

Muhammad Shafiq Ahmed
Graduate Student

**ELSEVIER LICENSE
TERMS AND CONDITIONS**

Aug 20, 2009

This is a License Agreement between Muhammad S Ahmed ("You") and Elsevier ("Elsevier") provided by Copyright Clearance Center ("CCC"). The license consists of your order details, the terms and conditions provided by Elsevier, and the payment terms and conditions.

All payments must be made in full to CCC. For payment instructions, please see information listed at the bottom of this form.

Supplier	Elsevier Limited
	The Boulevard,Langford Lane
	Kidlington,Oxford,OX5 1GB,UK
Registered Company Number	1982084
Customer name	Muhammad S Ahmed
Customer address	7 Prouse Drive
	Brampton, ON L6V3A3
License Number	2237740028792
License date	Jul 28, 2009
Licensed content publisher	Elsevier
Licensed content publication	Materials Science and Engineering: B
Licensed content title	Characterization methods of carbon nanotubes: a review
Licensed content author	T. Belin and F. Epron
Licensed content date	25 May 2005
Volume number	
Issue number	

Pages	0
Type of Use	Thesis / Dissertation
Portion	Full article
Format	Both print and electronic
You are an author of the Elsevier article	No
Are you translating?	No
Order Reference Number	1
Expected publication date	Aug 2009
Elsevier VAT number	GB 494 6272 12
Permissions price	0.00 USD
Value added tax 0.0%	0.00 USD
Total	0.00 USD

Terms and Conditions

INTRODUCTION

1. The publisher for this copyrighted material is Elsevier. By clicking "accept" in connection with completing this licensing transaction, you agree that the following terms and conditions apply to this transaction (along with the Billing and Payment terms and conditions established by Copyright Clearance Center, Inc. ("CCC"), at the time that you opened your Rightslink account and that are available at any time at http://myaccount.copyright.com).

GENERAL TERMS

2. Elsevier hereby grants you permission to reproduce the aforementioned material subject to the terms and conditions indicated.

3. Acknowledgement: If any part of the material to be used (for example, figures) has appeared in our publication with credit or acknowledgement to another source, permission must also be sought from that source. If such permission is not obtained then that material may not be included in your publication/copies. Suitable acknowledgement to the source must be made, either as a footnote or in a reference list at the end of your publication, as follows:

"Reprinted from Publication title, Vol /edition number, Author(s), Title of article / title of chapter, Pages No., Copyright (Year), with permission from Elsevier [OR APPLICABLE SOCIETY COPYRIGHT OWNER]." Also Lancet special credit - "Reprinted from The Lancet, Vol. number, Author(s), Title of article, Pages No., Copyright (Year), with permission from Elsevier."

4. Reproduction of this material is confined to the purpose and/or media for which permission is hereby given.

5. Altering/Modifying Material: Not Permitted. However figures and illustrations may be altered/adapted minimally to serve your work. Any other abbreviations, additions, deletions and/or any other alterations shall be made only with prior written authorization of Elsevier Ltd. (Please contact Elsevier at permissions@elsevier.com)

6. If the permission fee for the requested use of our material is waived in this instance, please be advised that your future requests for Elsevier materials may attract a fee.

7. Reservation of Rights: Publisher reserves all rights not specifically granted in the combination of (i) the license details provided by you and accepted in the course of this licensing transaction, (ii) these terms and conditions and (iii) CCC's Billing and Payment terms and conditions.

8. License Contingent Upon Payment: While you may exercise the rights licensed immediately upon issuance of the license at the end of the licensing process for the transaction, provided that you have disclosed complete and accurate details of your proposed use, no license is finally effective unless and until full payment is received from you (either by publisher or by CCC) as provided in CCC's Billing and Payment terms and conditions. If full payment is not received on a timely basis, then any license preliminarily granted shall be deemed automatically revoked and shall be void as if never granted. Further, in the event that you breach any of these terms and conditions or any of CCC's Billing and Payment terms and conditions, the license is automatically revoked and shall be void as if never granted. Use of materials as described in a revoked license, as well as any use of the materials beyond the scope of an unrevoked license, may constitute copyright infringement and publisher reserves the right to take any and all action to protect its copyright in the materials.

9. Warranties: Publisher makes no representations or warranties with respect to the licensed material.

10. Indemnity: You hereby indemnify and agree to hold harmless publisher and CCC,

and their respective officers, directors, employees and agents, from and against any and all claims arising out of your use of the licensed material other than as specifically authorized pursuant to this license.

11. No Transfer of License: This license is personal to you and may not be sublicensed, assigned, or transferred by you to any other person without publisher's written permission.

12. No Amendment Except in Writing: This license may not be amended except in a writing signed by both parties (or, in the case of publisher, by CCC on publisher's behalf).

13. Objection to Contrary Terms: Publisher hereby objects to any terms contained in any purchase order, acknowledgment, check endorsement or other writing prepared by you, which terms are inconsistent with these terms and conditions or CCC's Billing and Payment terms and conditions. These terms and conditions, together with CCC's Billing and Payment terms and conditions (which are incorporated herein), comprise the entire agreement between you and publisher (and CCC) concerning this licensing transaction. In the event of any conflict between your obligations established by these terms and conditions and those established by CCC's Billing and Payment terms and conditions, these terms and conditions shall control.

14. Revocation: Elsevier or Copyright Clearance Center may deny the permissions described in this License at their sole discretion, for any reason or no reason, with a full refund payable to you. Notice of such denial will be made using the contact information provided by you. Failure to receive such notice will not alter or invalidate the denial. In no event will Elsevier or Copyright Clearance Center be responsible or liable for any costs, expenses or damage incurred by you as a result of a denial of your permission request, other than a refund of the amount(s) paid by you to Elsevier and/or Copyright Clearance Center for denied permissions.

LIMITED LICENSE

The following terms and conditions apply to specific license types:

15. **Translation**: This permission is granted for non-exclusive world **English** rights only unless your license was granted for translation rights. If you licensed translation rights you may only translate this content into the languages you requested. A professional translator must perform all translations and reproduce the content word for word preserving the integrity of the article. If this license is to re-use 1 or 2 figures then permission is granted for non-exclusive world rights in all languages.

16. **Website**: The following terms and conditions apply to electronic reserve and author websites:

Electronic reserve: If licensed material is to be posted to website, the web site is to be password-protected and made available only to bona fide students registered on a relevant course if:

This license was made in connection with a course,

This permission is granted for 1 year only. You may obtain a license for future website posting,

All content posted to the web site must maintain the copyright information line on the bottom of each image,

A hyper-text must be included to the Homepage of the journal from which you are licensing at http://www.sciencedirect.com/science/journal/xxxxx or, for books, to the Elsevier homepage at http://www.elsevier.com,

Central Storage: This license does not include permission for a scanned version of the material to be stored in a central repository such as that provided by Heron/XanEdu.

17. **Author website** for journals with the following additional clauses:

All content posted to the web site must maintain the copyright information line on the bottom of each image, and

The permission granted is limited to the personal version of your paper. You are not allowed to download and post the published electronic version of your article (whether PDF or HTML, proof or final version), nor may you scan the printed edition to create an electronic version. A hyper-text must be included to the Homepage of the journal from which you are licensing at http://www.sciencedirect.com/science/journal/xxxxx, Central Storage: This license does not include permission for a scanned version of the material to be stored in a central repository such as that provided by Heron/XanEdu.

18. **Author website** for books with the following additional clauses:

Authors are permitted to place a brief summary of their work online only. A hyper-text must be included to the Elsevier homepage at http://www.elsevier.com. All content posted to the web site must maintain the copyright information line on the bottom of each image. You are not allowed to download and post the published electronic version of your chapter, nor may you scan the printed edition to create an electronic version. Central Storage: This license does not include permission for a scanned version of the material to be stored in a central repository such as that provided by Heron/XanEdu.

19. **Website** (regular and for author): A hyper-text must be included to the Homepage of the journal from which you are licensing at http://www.sciencedirect.com/science/journal/xxxxx or, for books, to the Elsevier homepage at http://www.elsevier.com.

20. **Thesis/Dissertation**: If your license is for use in a thesis/dissertation your thesis may be submitted to your institution in either print or electronic form. Should your thesis be published commercially, please reapply for permission. These requirements include permission for the Library and Archives of Canada to supply single copies, on demand, of the complete thesis and include permission for UMI to supply single copies, on demand, of the complete thesis. Should your thesis be published commercially, please reapply for permission.

21. **Other conditions:** None

v1.5

Gratis licenses (referencing $0 in the Total field) are free. Please retain this printable license for your reference. No payment is required.

If you would like to pay for this license now, please remit this license along with your payment made payable to "COPYRIGHT CLEARANCE CENTER" otherwise you will be invoiced within 30 days of the license date. Payment should be in the form of a check or money order referencing your account number and this license number 2237740028792.
If you would prefer to pay for this license by credit card, please go to http://www.copyright.com/creditcard to download our credit card payment authorization form.

Make Payment To:
Copyright Clearance Center
Dept 001
P.O. Box 843006
Boston, MA 02284-3006

If you find copyrighted material related to this license will not be used and wish to cancel, please contact us referencing this license number 2237740028792 and noting the reason for cancellation.

Questions? customercare@copyright.com or +1-877-622-5543 (toll free in the US) or +1-978-646-2777.

Email: info@copyright.com
Subject: Copyright permission

Date:July 27, 2009

Publisher: CRC Press LLC, 2000 N.W. Corporate Blvd., Boca Raton, Florida 33431

Dear Editor,
I am preparing my M.Sc. thesis for submission to the Office of Graduate Studies at the University of Ontario Institute of Technology (UOIT) in Oshawa, Ontario, Canada. I am seeking your permission to include a manuscript version of the following figures in the thesis:

1. Carbon nanotubes : science and applications / edited by M. Meyyappan, © 2005 by CRC Press LLC.
   Figure 1.1 on page 3
   Figure 1.4 on page 5
   Figure 5.9 on page 126

2. Introduction to Nanotechnology / by Gabor Louis Hornyak , © 2008 by CRC Press LLC.
   Figure 3.6 on page 131
   Figure 3.9 on page 136
   Figure 9.25 on page 478

3. Nanomanufacturing Handbook, edited by Ahmed Busnaina, © 2007 Taylor & Francis Group, LLC
   Figure 4.3 on page 84.

Canadian graduate theses are reproduced by the Library and Archives of Canada (formerly National Library of Canada) through a non-exclusive, world-wide license to reproduce, loan, distribute, or sell theses. I am also seeking your permission for the material described above to be reproduced and distributed by the LAC(NLC). Further details about the LAC(NLC) thesis program are available on the LAC(NLC) website (www.nlc-bnc.ca).
Full publication details and a copy of this permission letter will be included in the thesis.
Yours sincerely,

Muhammad Shafiq Ahmed
Graduate Student

© COPYRIGHT CLEARANCE CENTER

Confirmation Number: 2142671
Order Date: 07/28/2009

Customer Information

Customer: Muhammad Ahmed
Account Number: 3000188953
Email: muhammadshafiq.ahmed@uoit.ca
Phone: +1 (416) 230-3072
Payment Method: Invoice
PO#: 2

CARBON NANOTUBES: SCIENCE AND APPLICATIONS
Order detail ID: 28378605

ISBN/ISSN: 978-0-8493-2111-5
Publication Year: 2004
Publisher: CRC PRESS LLC
Rightsholder: Taylor & Francis Group LLC - Books
Author/Editor: M. Meyyappan

Permission Status: ✅ **Granted**
Comment: Please check copyright line before republishing.
Permission type: Republish into a book, journal, newsletter…
Requested use: Dissertation
Republishing organization: UNIVERSITY OF ONTARIO INSTITUTE OF TECHNOLOGY
Organization status: Not for profit
Republication date: 08/25/2009
Circulation/Distribution: 5
Type of content: Figure, diagram, or table
Description of requested content: FIGURE 1.1 Bonding structures of diamond, graphite, nanotubes, and fullerenes, FIGURE 1.4 By rolling a graphite sheet in different directions, FIGURE 5.9 Raman active eigenmodes along with their frequencies for a (10,10) nanotube
Page range(s): 3,5,
Requested content's publication date: 01/01/2004

NANOMANUFACTURING HANDBOOK
Order detail ID: 28378604

ISBN/ISSN: 978-0-8493-3326-2

Permission Status: ✅ **Granted**
Comment: Please check copyright line before republishing.

Publication Year: 2006
Publisher: TAYLOR &
FRANCIS GROUP LLC
Rightsholder: Taylor &
Francis Group LLC -
Books
Author/Editor: Yung
Joon Jung

Fee waived because material being used in dissertation.
Permission type: Republish into a book, journal,
newsletter…
Requested use: Dissertation
Republishing organization: UNIVERSITY OF ONTARIO
INSTITUTE OF TECHNOLOGY, OSHAWA, ON
Organization status: Not for profit
Republication date: 08/25/2009
Circulation/Distribution: 5
Type of content: Figure, diagram, or table
Description of requested content: Fig. 4.3
Page range(s): 84
Requested content's publication date: 01/01/2006

INTRODUCTION TO NANOSCIENCE
Order detail ID: 28378603

ISBN/ISSN: 978-1-4200-
4805-6
Publication Year: 2008
Publisher: TAYLOR &
FRANCIS GROUP LLC
Rightsholder: Taylor &
Francis Group LLC -
Books
Author/Editor: Gabor L.
Hornyak

Permission Status: ✓ **Granted**
Comment: Please check copyright line before republishing.
Fee waived because material will be used in a dissertation
Permission type: Republish into a book, journal,
newsletter…
Requested use: Dissertation
Republishing organization: UNIVERSITY OF ONTARIO
INSTITUTE OF TECHNOLOGY, OSHAWA, ON
Organization status: Not for profit
Republication date: 08/25/2009
Circulation/Distribution: 5
Type of content: Figure, diagram, or table
Description of requested content: Fig. 3.6 A scematic
diagram of SEM, Fig. 3.9 A schematic diagram of TEM,
Fig. 9.25 Phase diagram of carbon materials
Page range(s): 131, 136, 478
Requested content's publication date: 01/01/2008

Dear Muhammad,

Taylor & Francis hereby grants you permission to reprint Figure 1.1 of CARBON NANOTUBES: SCIENCE AND APPLICATIONS 978-0-8493-2111-5, Figure 4.3 of NANOMANUFACTURING HANDBOOK 978-0-8493-3326-2, Figures 3.6, 3.9 and 9.25 of INTRODUCTION TO NANOSCIENCE 978-1-4200-4805-6 in a graduate thesis to be re-printed in the Library and Archives of Canada.

Permission is given on a one-time, nonexclusive basis. Future uses of the material must be applied permission for.

Best Regards,

Mindy Rosenkrantz
Permissions Coordinator
Taylor and Francis Group
270 Madison Avenue 4th Floor
New York, NY 10016
Permissions.Mailbox@taylorandfrancis.com